UNITED STATES ENVIRONMENTAL PROTECTION AGENCY
RESEARCH TRIANGLE PARK, NC 27711

AUG 15 2012

OFFICE OF
AIR QUALITY PLANNING
AND STANDARDS

MEMORANDUM

SUBJECT: Model-based rollback using the higher order decoupled direct method (HDDM)

FROM: Heather Simon OAR/OAQPS/AQAD
Kirk Baker, OAR/OAQPS/AQAD
Norm Possiel, OAR/OAQPS/AQAD
Farhan Akhtar, OAR/OAQPS/HEID
Sergey Napelenok, ORD/NERL/AMAD
Brian Timin, OAR/OAQPS/AQAD
Benjamin Wells, OAR/OAQPS/AQAD

TO: EPA Docket # EPA–HQ–OAR–2008–0699

As part of the reviews of the National Ambient Air Quality Standards (NAAQS) for ozone, EPA estimates health risks after ozone has been adjusted to just meet the current standard and alternative standards. The first draft documents for this review rely upon the quadratic rollback method used in previous reviews to adjust or "roll back" hourly ozone concentrations in urban areas. Although the quadratic rollback method simulates historical patterns of air quality changes better than some alternative methods (e.g. simply shaving peak concentrations off at the NAAQS level), its implementation requires some assumptions that may not always hold true. EPA has received comments during past ozone NAAQS reviews and during the January 9-10, 2012 Clean Air Scientific Advisory Committee (CASAC) meeting for this ozone NAAQS review which encourage the use of alternate methods to quadratic rollback. In addition, the National Research Council of the National Academies (NRC, 2008) recommended that EPA explore how emissions reductions might effect temporal and spatial variations in O_3 concentrations, and to include information on how NO_x versus VOC control strategies might affect risk and exposure to O_3. In the attachment to this memo we present a model-based ozone adjustment approach. This analysis uses the CMAQ photochemical model instrumented with

the higher order direct decoupled method (HDDM) - an approach that generates modeled sensitivities of ozone to emissions changes - to estimate ozone concentrations that would occur with the achievement of a 0.075 ppm ozone standard in multiple urban areas.

Based on the analysis presented here, we believe that there are clear benefits for using the model-based adjustments for the second draft REA. For example, the HDDM model-based adjustment approach, unlike quadratic rollback, allows us to predict temporally- and spatially-varying response within an urban area to emissions changes and allows us to account for the sensitivity of air quality changes to NOx versus VOC emissions reductions. For example, model-based adjustments account for ozone increases with NOx reductions which may occur at times and locations where NOx to VOC ratios are high and total ozone concentrations are low. This approach also directly accounts for physical and chemical processes that lead to ozone formation and transport and includes natural and anthropogenic sources of ozone precursors from sources both within and outside of the U.S. Consequently, it is more straightforward to isolate the ozone response to U.S. emission reductions, eliminating the need to artificially specify a floor for air quality changes as is required in the quadratic rollback method. Compared to quadratic rollback, the capabilities of the HDDM model-based adjustment approach build confidence that the results drawn from this type of analysis allow us to more realistically represent the response in hourly ozone concentrations to reductions in emissions for a scenario of just meeting the current and alternative standard levels. Further analyses will be conducted to better understand the effect of using the HDDM model-based adjustment approach on the results of the risk and exposure assessment.

Attachment

Attachment
Model-based rollback using the higher order decoupled direct method (HDDM)

Table of Contents

Table of Figures

Table of Tables

1. MOTIVATION FOR A NEW TECHNIQUE TO SIMULATE OZONE CONCENTRATIONS UNDER ALTERNATIVE STANDARDS

As part of the reviews of the National Ambient Air Quality Standards (NAAQS) for ozone, EPA estimates health risks after ozone has been adjusted to just meet the current standard and alternative standards. The first draft documents for this review rely upon the quadratic rollback method used in previous reviews to adjust or "roll back" hourly ozone concentrations in urban areas. Although the quadratic rollback method simulates historical patterns of air quality changes better than some alternative methods (e.g. simply shaving peak concentrations off at the NAAQS level), its implementation requires some assumptions that may not always hold true. First, the quadratic rollback method requires that all monitors in an urban area exhibit the same response to emissions changes not allowing for temporally varying response depending on time of day. In addition, it assumes that ozone concentrations never increase in response to emissions reductions. However, during NOx-saturated (VOC limited) conditions, NOx reductions can result in ozone increases (Seinfeld and Pandis, 1998). Finally, since the quadratic rollback method is purely a mathematical technique and does not account for physical and chemical atmospheric processes or the sources of emissions precursors that lead to ozone formation, a backstop or "floor" must be used to ensure that predicted ozone is not reduced below "background" concentrations[1].

EPA has received comments during past ozone NAAQS reviews and during the January 9-10, 2012 Clean Air Scientific Advisory Committee (CASAC) meeting for this ozone NAAQS review which encourage the use of alternate methods to quadratic rollback. In addition, the National Research Council of the National Academies (NRC, 2008) recommended that EPA explore how emissions reductions might effect temporal and spatial variations in O_3 concentrations, and to include information on how NO_x versus VOC control strategies might affect risk and exposure to O_3.

Photochemical modeling can simulate the ozone response to emission reductions while avoiding the limitations presented by the quadratic rollback method. While there are uncertainties inherent in any modeling exercise due to uncertainties in inputs and model parameters, the improved characterization of the spatial and temporal responses of ozone to the

[1] Background ozone has been characterized in previous reviews of the ozone NAAQS as "policy relevant background" or PRB, defined as ozone concentrations that would exist in the absence of North American anthropogenic emissions. In the current review, we have refined the concept of background ozone to recognize that there are several possible definitions of background ozone, reflecting both the geographic source of emissions, e.g. U.S., North American, Global non-U.S., and whether emissions are anthropogenic or natural in origin. In the cases described in this document, "background" refers to ozone that would exist in absence of U.S. anthropogenic emissions.

reductions in emissions that would be needed to just meet the standards justify these additional uncertainties. In this document we present a model-based ozone adjustment approach. This analysis uses the CMAQ photochemical model instrumented with the higher order direct decoupled method (HDDM) - an approach that generates modeled sensitivities of ozone to emissions changes - to estimate ozone concentrations that would occur with the achievement of a 0.075 ppm ozone standard in multiple urban areas. This modeling incorporates all known emissions, including emissions from non-anthropogenic sources and anthropogenic emissions from sources in and outside of the U.S. As a result, the need to specify values for U.S. background concentrations is not necessary, as it is incorporated in the modeling directly. Because the simulations focus on reductions in U.S. anthropogenic emissions while holding constant those emissions that influence U.S. background, all changes in ozone will be relative to U.S. background. This does not mean that the background ozone concentrations will be constant between recent ambient ozone conditions and after just meeting the current standards, because of nonlinearities in the formation of ozone. In simulations of just meeting the standards used to inform the exposure and risk assessment, HDDM sensitivities can be applied relative to ambient measurements of O_3 to estimate how ozone concentrations would respond to changes in anthropogenic emissions within the U.S. We propose to use this methodology to simulate ozone concentrations meeting the current and alternative standards in the 2nd drafts of the risk and exposure assessments and the 2nd draft policy assessment.

2. HIGHER ORDER DECOUPLED DIRECT METHOD (HDDM)

Chemical transport models, such as the Community Multiscale Air Quality Model (CMAQ) (www.cmaq-model.org), calculate the effects of physical and chemical processes in the atmosphere to predict 3-D gridded pollutant concentrations (Foley et al, 2011, Appel et al, 2008, Appel et al, 2007, Byun and Schere, 2006). These models account for the impacts of emissions, transport, chemistry, and deposition on spatially and temporally varying pollutant concentrations. Required model inputs include time-varying emissions and meteorology fields, time varying concentrations of pollutants at the boundaries of the model domain (i.e. boundary conditions), and a characterization of the 3-D field of chemical concentrations to initialize the model (i.e. initial conditions). A simplified version of the atmospheric diffusion equation solved by such models is given in Equation (1) (Cohan and Napelenok, 2011):

$$\frac{\partial C_i}{\partial t} = -\nabla(uC_i) + \nabla(K\nabla C_i) + R_i + E_i + \cdots \qquad \text{Equation (1)}$$

In this equation (which is defined to vary in both space and time), C_i represents the atmospheric concentration field of compound i, u gives the wind field, K represents the turbulent diffusivity tensor, R_i is a represents the net rate of chemical production (which encompasses gas, aqueous, and particle reactions), E_i represents the emissions rate, and the ellipsis shows that other processes are also accounted for in the model (such as deposition, particle coagulation, and partitioning of semivolatile species between gas and particle phases). Solving Equation (1) is complicated by the fact that these models include many chemical species whose concentrations are interconnected through the R_i and partitioning terms.

Chemical transport models include sources outside of US control which are often termed "background" and explicitly account for transport of pollutants from outside the model domain and emission of pollution precursors from natural and anthropogenic sources within the model domain. Beyond modeling the current concentrations of ambient ozone, chemical transport models can be used to estimate the response of ambient ozone concentrations to changes in emissions.

One technique to model this response, the brute force method, requires the modeler to explicitly model this response by directly altering the emissions inputs in the model simulation. This technique provides an accurate estimate of the ozone concentration at the altered emission level, but often does not provide accurate information regarding the response of ozone to other levels of emissions since the chemistry for ozone formation is nonlinear. Therefore, when using only brute force techniques a new model simulation would need to be performed for every emissions scenario in question.

Other analytical techniques have been developed to estimate the ozone response to emissions perturbations without rerunning the entire simulation. One such method is termed the decoupled direct method (DDM) (Dunker 1984). DDM, solves for sensitivity coefficients which are defined as the partial derivative of the atmospheric diffusion equations that underly the model calculations, Equations (2) and (3).

$$\boldsymbol{s_{ij}(t)} = \frac{\partial \boldsymbol{C_i(t)}}{\partial \boldsymbol{p_j}} \qquad \text{Equation (2)}$$

$$\boldsymbol{S_{ij}(t)} = \widetilde{\boldsymbol{P}}_{\boldsymbol{j}} \frac{\partial \boldsymbol{C_i(t)}}{\partial \boldsymbol{p_j}} = \widetilde{\boldsymbol{P}}_{\boldsymbol{j}} \frac{\partial \boldsymbol{C_i(t)}}{\partial (\epsilon_j \widetilde{\boldsymbol{P}}_{\boldsymbol{j}})} = \frac{\partial \boldsymbol{C_i(t)}}{\partial \epsilon_j} \qquad \text{Equation (3)}$$

Here, $s_{ij}(t)$, the sensitivity, gives the change in model concentration, C_i, (for instance ozone concentration) with an incremental change in any input parameter, p_j (in this case emissions). Equation (3) allows us to normalize the sensitivity coefficient, $S_{ij}(t)$, so that it shows response in relative terms for the input rather than in absolute units. Therefore, $\tilde{P}_j$ (x,t) is the normalized

input and ε_j is a scaling variable (Yang et al, 1997). In general terms, the sensitivity coefficient tells us how a model output (ozone concentration) will change if a model input (emissions of NO_x or VOC) is perturbed. This first order sensitivity coefficient, $S_{ij}(t)$ is quite accurate for small perturbations, but gives a linear response which is not accurate for large perturbations in very nonlinear relationships. Second (and third) order derivatives can be taken to give higher order sensitivity coefficients (Hakami et al, 2003). Higher order sensitivity coefficients give the curvature and inflection points for the response curve and can capture the nonlinearities in the response of ozone to emissions changes. Using higher order DDM (HDDM) allows for the sensitivities to be accurately applied over larger emissions perturbations. Hakami et al. (2003) report that for an application in California, HDDM gave good approximations of ozone changes for perturbations of emissions up to 50% using the first three terms of the Taylor series expansion, Equation (4).

$$\boldsymbol{C}(+\Delta\boldsymbol{\epsilon}) = \boldsymbol{C}(\mathbf{0}) + \Delta\boldsymbol{\epsilon}\boldsymbol{S}(\mathbf{0}) + \frac{\Delta\epsilon^2}{2}\boldsymbol{S}^{\mathbf{2}}(\mathbf{0}) + \ \ldots + \frac{\Delta\epsilon^n}{n!}\boldsymbol{S}^{\boldsymbol{n}}(\mathbf{0}) + \boldsymbol{R}_{\boldsymbol{n+1}} \qquad \text{Equation (4)}$$

Here $\Delta\epsilon$ represents the relative change in emissions (for instance $\Delta\epsilon$ = -0.2 would be equivalent to reducing emissions by 20%), $S^n(0)$ is the n-th order sensitivity coefficient, C(0) is the concentration under baseline conditions (no perturbation in emissions) and R_{n+1} is a remainder term.

2.1 CAPABILITIES

DDM and HDDM have been implemented into several chemical transport models for both ozone and particulate matter (PM) predictions (Dunker, 1984; Yang et al, 1997; Hakami et al, 2003; Cohan et al, 2005; Napelenok et al, 2006; Koo et al., 2010; Zhang et al, 2012). These implementations allow the modeler to define the parameters for which sensitivities will be calculated. For instance, the sensitivity can be calculated for emissions from a specific source type, for emissions in a specific geographic region, and for emissions of a single ozone precursor or for multiple ozone precursors. In addition, sensitivities can be calculated to boundary conditions, initial conditions, and various other model inputs. Sensitivities to different sets of parameters can be calculated in a single model simulation but computation time increases as the number of sensitivities increases. Outputs from an HDDM simulation consist of time varying 3-D fields of first and second order sensitivities.

For the purposes of the ozone NAAQS analysis, HDDM has the potential to provide an improved approach compared to current quadratic rollback techniques for several reasons. First, it captures non-linearity of ozone response to emissions changes, representing both increases and decreases in ozone concentrations resulting from emissions reductions. Second,

HDDM characterizes different ozone response at different locations (downtown urban versus downwind suburban) and at different times of day to emissions reductions allowing us to incorporate temporal and spatial variations in response into the ozone adjustment methodology. Finally, HDDM eliminates the need to use "background" ozone as a floor for rollback since predicted sensitivities are based on model formulations that explicitly account for background sources.

2.2 LIMITATIONS

In addition to the many potential benefits of using HDDM to understand ozone response to emissions changes, there are several limitations. First, HDDM encompasses all of the uncertainties of the base model formulation and inputs. So uncertainties in how the physical and chemical processes are treated in the model and in the model inputs propagate to the HDDM results. Also, HDDM can capture response to larger emissions perturbations than DDM but it is still most accurate for small perturbations. The larger the relative change in emissions, the less likely that the HDDM sensitivities will be capturing the change in ozone that would be predicted by a brute force model simulation. Several studies have reported reasonable performance of HDDM for ozone up to 50% emissions perturbations (Hakami et al, 2003; Cohan et al., 2005; Hakami et al, 2004), but the magnitude of perturbation over which HDDM will give accurate estimates will depend on the specific modeling episode, size of the model domain, emissions and meteorological inputs, and the size of the emissions source to which the sensitivity is being calculated. In this work, we applied sensitivities from simulations done under varying NOx levels (see Section 3.2.3) and found that using this technique we were able to replicate brute force estimates using HDDM sensitivities for up to 75% NOx or VOC reductions with a normalized mean bias of less than 10% and a normalized mean error of less than 15%.

3. USING HDDM/CMAQ FOR SIMULATIONS OF JUST MEETING ALTERNATIVE STANDARDS: METHODOLOGY

3.1 CONCEPTUAL FRAMEWORK

This section outlines the methodology applied to use CMAQ/HDDM to estimate hourly ozone concentrations that might result from meeting the current and possible new ozone NAAQS. Note that model results are not used in an absolute sense, but instead are applied to ambient measurements, thus tying predicted ozone distributions more directly to measured

values. The basic steps are outlined below and in Figure 1. Details are given in section 3.2 and Appendix A.

- **Step 1:** Run CMAQ simulation with HDDM to determine hourly ozone sensitivities to NO_x emissions and VOC emissions for the grid cells containing monitoring sites in an urban area.
- **Step 2:** For each monitoring site, group days by predicted daily 8-hr max ozone and predicted high versus low nighttime ozone. Calculate average diurnal profiles for sensitivities in each group.
- **Step 3:** For each monitoring site, assign one of the diurnal sensitivity profiles calculated in Step 2 to each day in the period 2006 through 2008[2] based on measured 8-hr max ozone and measured nighttime ozone.
- **Step 4:** Adjust measured hourly ozone concentrations for incrementally increasing levels of emissions reductions using assigned sensitivities and then recalculate design values until all monitors in an urban area are in attainment of current and proposed alternative levels of the standard.

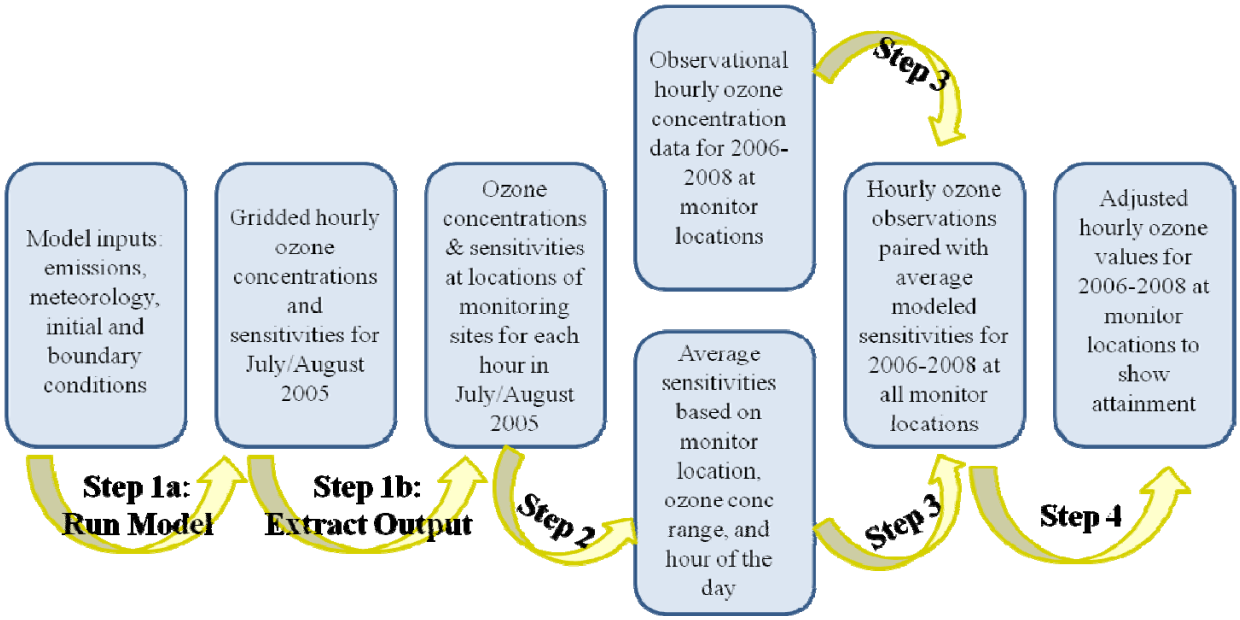

Figure 1: Flow diagram demonstrating DDM model-based ozone adjustment approach

[2] The first draft of the Health Risk and Exposure Assessment for the 2013 ozone NAAQS review (US EPA, 2012) estimated the health impacts of meeting various levels of the NAAQS for two three-year periods: 2006-2008 and 2008-2010. In this analysis we focus on the first of these three-year periods.

3.2 APPLICATION TO CASE STUDIES IN ATLANTA AND DETROIT

In this case study, we illustrate the model-based adjustment approach for attainment of the 75 ppb NAAQS. The analysis covers two cities (Atlanta and Detroit) using modeling for July and August 2005 and ambient data for the years 2006-2008. Atlanta and Detroit were chosen for this analysis because they are both cities included in exposure analysis and because they represent different chemical ozone formation regimes[3]. These case studies were selected as a proof-of-concept for the application of the HDDM model-based ozone adjustment approach. In addition, these case studies have helped us identify a number of challenges and the benefits of this type of approach.

3.2.1 Binning of HDDM sensitivities

When running CMAQ with HDDM additional inputs are required to designate model inputs for calculating sensitivities. In this analysis, HDDM was set up to calculate the sensitivity of ozone concentrations to domainwide (within the 12km Eastern domain – see Figure 16) anthropogenic NO_x and VOC emissions. US anthropogenic emissions were defined as all emissions in the following sectors: nonpt, nonroad, onroad, alm_no_c3, ptipm, ptnonipm, and seca_C3 (see Table 5) and accounted for 17,595,000 of the total domainwide 20,729,000 tons per year of NO_x emissions. Sensitivities were not determined for biogenic, fire, Canadian, or Mexican emissions. In addition, sensitivities were not calculated for any emissions originating from outside the domain (i.e. entering through the use of boundary concentrations).

First and second order hourly ozone sensitivities to VOC and NO_x were extracted from the HDDM simulation for model grid cells that contained one of ten ozone monitors near Atlanta, GA and one of eight ozone monitors near Detroit, MI. Maps of the Atlanta and Detroit area ozone monitor locations are shown in Figure 2 and Figure 3. The 18 monitors within these two areas are being used for this analysis because data availability was such that design values could be calculated for the years 2006-2008. Note that sites131210055 and 130890002 in Atlanta are contained in the same model grid cell and therefore are modeled as having the same sensitivities to NO_x and VOC emissions.

[3] Different sources of VOC and NO_x in the Midwest and Southeastern US lead to different VOC/NO_x ratios, ozone formation chemistry, and sensitivity to emissions changes in these two regions. Generally the large sources of biogenic VOC emissions in the Southeastern US have a large regional impact of ozone formation.

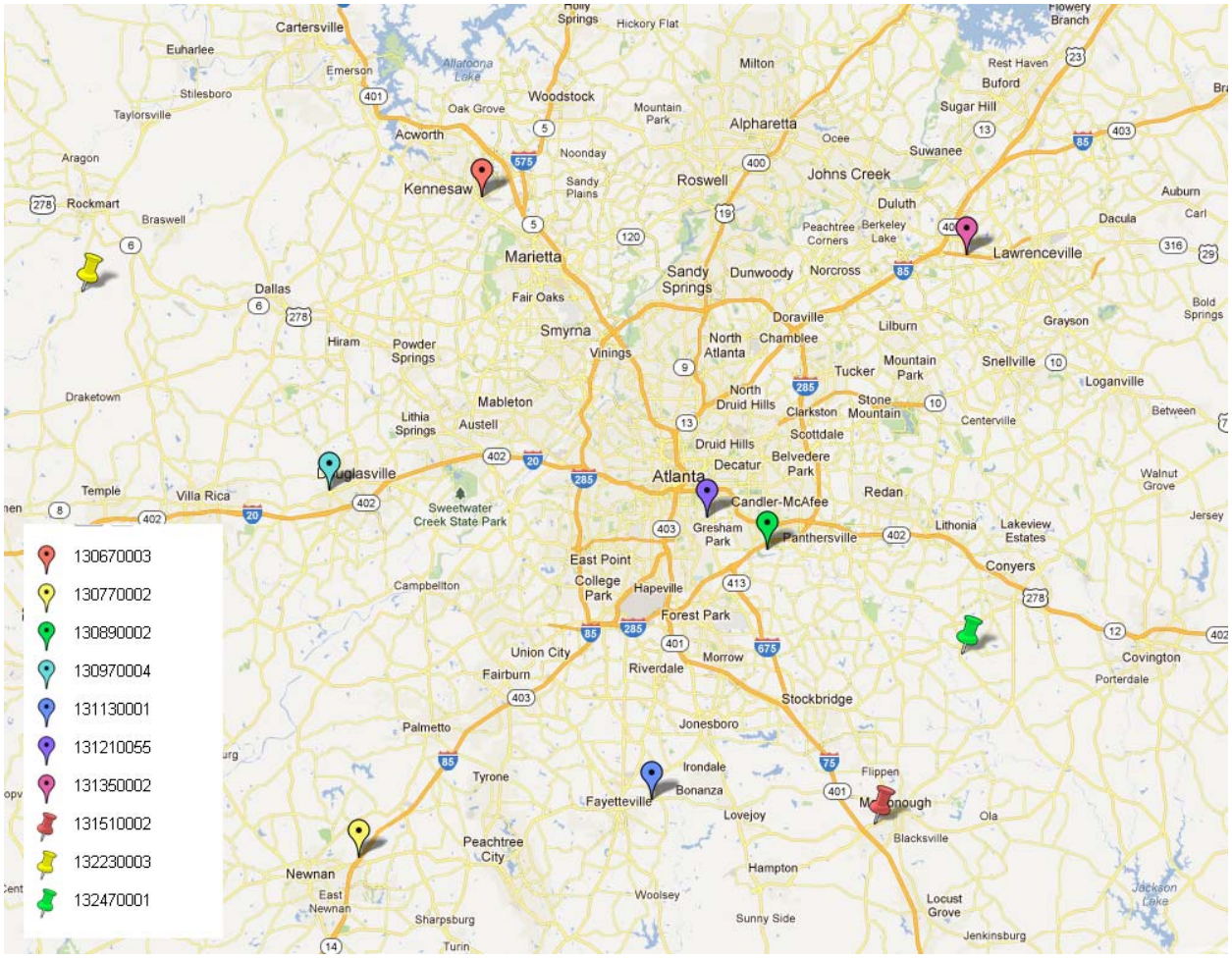

Figure 2: Map of ozone monitors in the Atlanta area used for this analysis

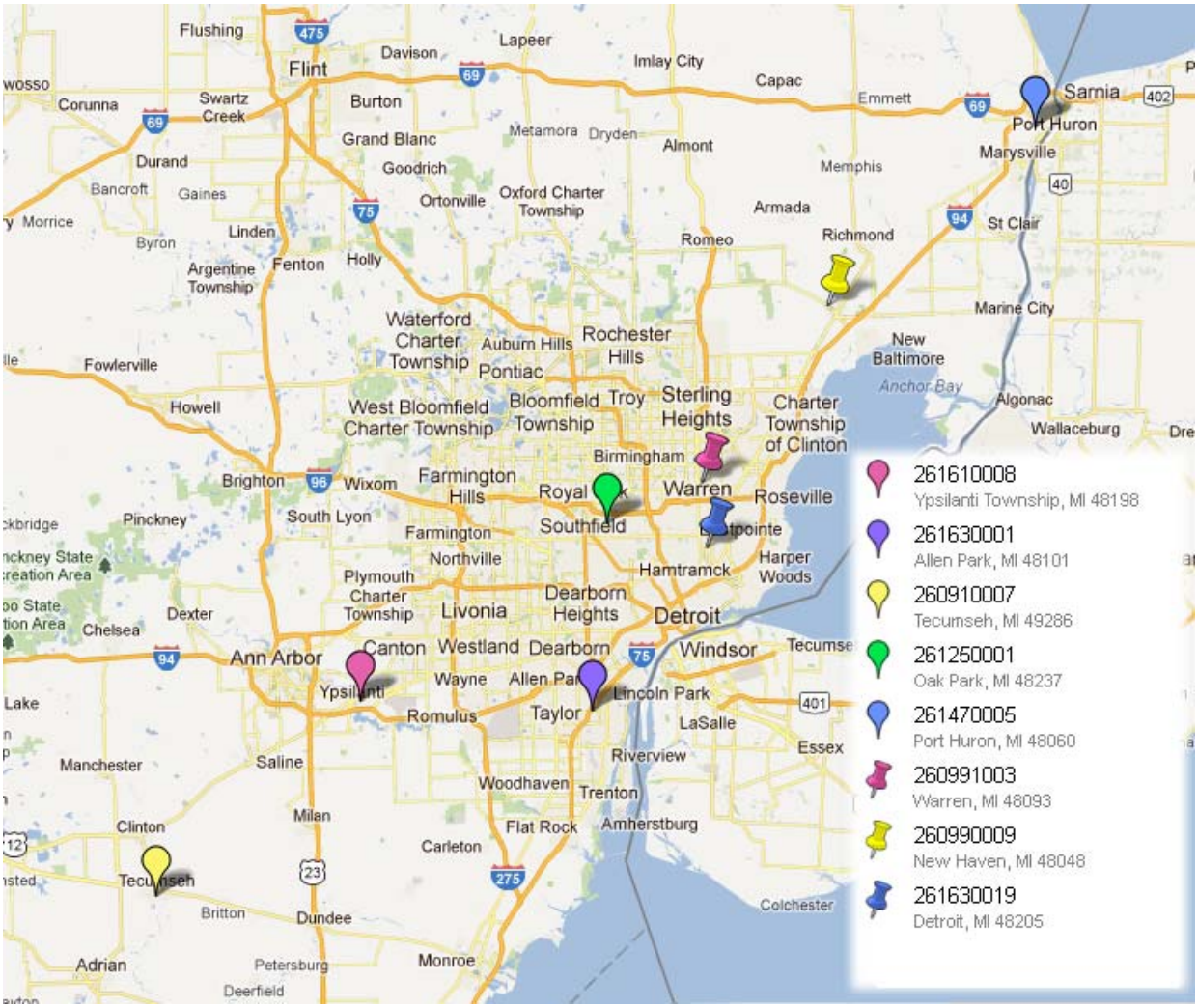

Figure 3: Map of ozone monitors in the Detroit area used for this analysis

Extracted data included modeled sensitivities at monitor locations for all hours in July and August 2005. These sensitivities cannot be applied directly to observed values for two reasons 1) high modeled ozone days/hours do not always occur concurrently with high observed ozone days/hours and 2) the modeling time period covers July and August 2005 but the time period we are analyzing in this proof-of-concept analysis is 2006-2008. As to the first point, photochemical models are generally used in a relative sense for purposes of projecting design values to assess attainment with the NAAQS standard. In this manner, model predictions are "anchored" to measured ambient values. This is generally not done on a day-specific basis, but instead average response on high modeled days is used for this purpose. This allows for more confidence in calculated results when "less than ideal model performance [occurs] on individual days" (US EPA, 2007). Similarly, for this analysis we believe it is appropriate to account for the fact the model does not always perfectly agree with

measurements and that sensitivities from a low-ozone modeled day would not be appropriate to apply to a high-ozone measured day (and vice-versa) even if they occur on the same calendar day. For the second point, due to current resource and time constraints we were only able to model two months in 2005 for the purposes of developing and testing the methodology. However, the ozone exposure analysis evaluates the effects of ozone decreases for two 3-year periods in 2006-2008 and 2008-2010. The analysis presented in this section only examines 2006-2008 ambient data, but this is still outside the modeled time period. For both of these reasons, a method was developed to generalize the modeled hour-specific sensitivities so that they could be applied to ambient data.

For each grid cell containing a monitor, each modeled day was classified based on its CMAQ-simulated daily 8-hr maximum ozone concentration. Five classifications were developed for days with 8-hr daily maximum ozone concentrations < 45 ppb, 45-55 ppb, 55-65 ppb, 65-75 ppb, and $\geq$ 75 ppb: each bin includes values at the lower limit but not at the upper limit (i.e. for the 44-55 bin, days are included that are $\geq$ 45 and < 55). The rational for this binning system is that the response of ozone to emissions reductions will be greater when ozone concentrations themselves are higher (see Figure 4). From these groupings, five average diurnal sensitivity profiles were created for each monitor location and for each sensitivity type (first order NO_x, second order NO_x, first order VOC, and second order VOC). These average sensitivities were calculated by taking the median sensitivity of all modeled sensitivities at a particular hour for the group of days falling within a bin (i.e. the median for all 8 am hours on days < 45 ppb would be used as a "typical" 8 am response for this lowest bin, the median for all 9 am hours on those days would be used as a "typical" 9 am response, etc.). Days were defined as running from 6 am to 5 am so that the 1 am – 5 am sensitivities were binned based on the previous day's 8-hr maximum ozone concentration.

The median values described above are meant to capture the "typical" response at each site based on 8-hr maximum ozone. However, there is variation among the sensitivities from the days that comprise each binned group, especially during nighttime hours. In general, nights with higher ozone concentrations within each bin are also more responsive to emissions reductions. Consequently, nighttime hours within each bin are further classified by "high" versus "low" nighttime ozone. For the purposes of this analysis, nights with at least one hourly ozone concentration above 50 ppb (between 7 pm and 5 am) are classified as high ozone nights. Sensitivities for nighttime hours (7 pm to 5 am) use median values from only "high" or "low" ozone nights within the original bin, while sensitivities for daytime hours (6 am to 6 pm) use median values from all days in the original bin. For bins and sites that contain only "high" or only "low" nights, sensitivities for nighttime values are also calculated as the median from all nighttime hours in the original bin.

Figure 4a presents the diurnal profiles for site 13121005 in downtown Atlanta on high ozone nights and shows the calculated change in ozone for each bin that would occur with a 30% decrease in NO_x emissions (using both the first and second order sensitivity terms). Figure 4b shows the same information as Figure 4a but for low ozone nights. Several features are evident in these plots. First, as described above, there is more ozone response (larger decrease in predicted ozone concentration) on days with higher 8-hr maximum ozone values. Second, while the model predicts ozone decreases during daytime hours, there are clear disbenefits (ozone increases) during morning and evening rush hour times (although the degree of this disbenefit and the length of time it lasts depend on the ozone bin). For this site, the days in the highest and lowest 8-hr maximum ozone bins also have higher peak ozone increases during morning and evening hours than is seen on mid-range ozone days. Also, for site 131210055 there were no high ozone nights in the <45, 45-55, and 55-65 ppb bins so the nighttime responses in Figure 4a and Figure 4b are the same for those bins. As explained above, the high ozone nights (Figure 4a) show smaller disbenefits and/or larger ozone decreases than low ozone nights (Figure 4b) between 7 pm and 5 am. This behavior varies by site. VOC response is similar in that high ozone bins generally have more response. However, no disbenefits occur in the VOC sensitivities. Figures shown here are for one site and only for response to NO_x emissions changes. Figures for all other Atlanta sites (NO_x sensitivities only) and all Detroit sites (NO_x and VOC sensitivities) are shown in Section Appendix B of this document.

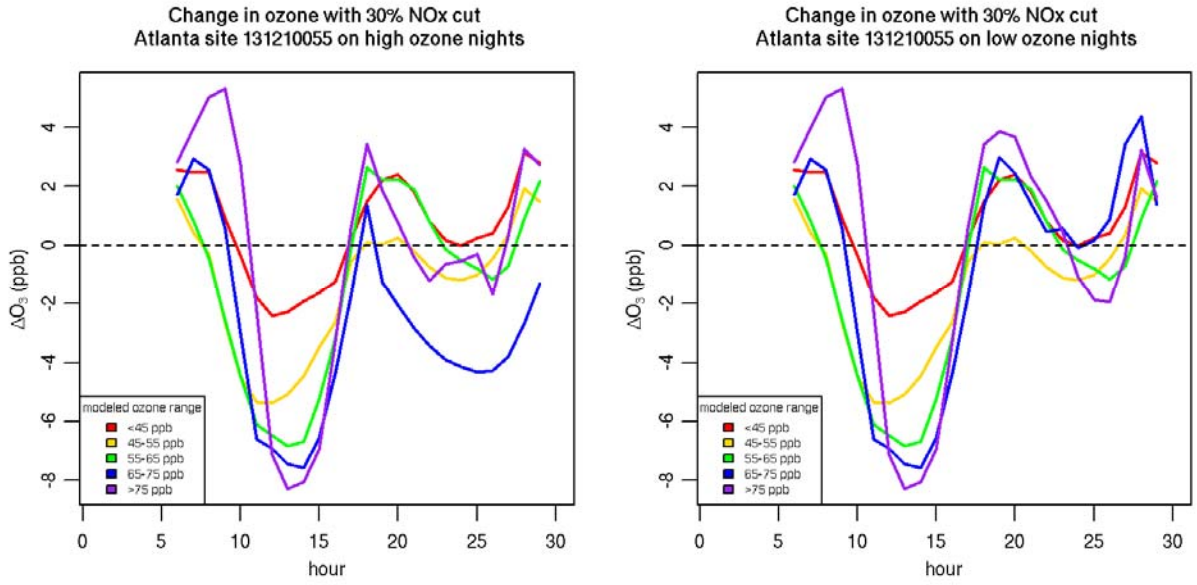

Figure 4: Predicted change in ozone concentrations (ppb) at Atlanta site 131210055 with a 30% decrease in US anthropogenic NO_x emissions in the Eastern US domain based on bins created for high ozone nights (left) and on bins created for low ozone nights (right). Hours 25-29 represent 1 am – 5 am the following morning.

3.2.2 Application of binned sensitivities to ambient data

To apply the binned sensitivity profiles to ambient data, each day from each monitor for 2006-2008 was grouped by measured 8-hr maximum ozone and high versus low nighttime ozone. The binning criteria were identical to that used for creating the average diurnal sensitivity profiles except that ambient ozone values were used in place of modeled ozone values. Each day at each monitor was then assigned to an average diurnal sensitivity profile from the appropriate bin. Note that if no measurements were taken for a particular day or if not enough hourly ozone concentrations were measured to calculate a valid maximum daily 8-hr ozone concentration then no sensitivity profile was assigned (for 1 am – 5 am the 8-hr maximum ozone concentration was needed from the previous day). Once each hour at each monitor was assigned an average sensitivity, the response at that monitor to changes in NO_x or VOC emissions could be calculated.

To perform the model-based ozone adjustments, each urban area was treated separately. Within an urban area, we used the binned sensitivities to determine the impacts on hourly ozone for incrementally increasing emissions reductions (NO_x or VOC). The same emissions reductions were applied to the sensitivity profiles for all monitors within the urban area and over all hours for each day. Each incremental reduction leads to a new set of hourly ozone concentrations for all days from 2006-2008 at each monitor. After each increment, 8-hr maximum daily ozone values were recalculated for each day. Adjusted design values were then calculated based on the 3-year average of the 4^{th} highest 8-hr maximum value at each site. The emissions reduction was incrementally increased until all monitors within an urban area were predicted to have design values below 75 ppb. If no sensitivity was assigned to a particular hour and monitor (due to lack of 8-hr daily max ozone classification), then a missing value was assigned to the adjusted ozone value. Note that since 1 am-5 am hours depend on the presence of an 8-hr maximum ozone concentration from the previous day, there may be more missing values in the HDDM-based adjusted ozone values than in the measured ozone values or in the quadratic rollback case.

3.2.3 Multi-step application of HDDM sensitivities

As discussed in Section 2.2 of this document, HDDM has been reported to reasonably replicate brute force emissions reductions up to a 50% change in emissions. For this analysis, it was desirable to have confidence that the HDDM sensitivities could replicate the entire range of emissions reductions. Evaluations of the HDDM estimates compared to brute force zero out model runs in Detroit and Atlanta showed that the HDDM estimates of ozone response to VOC emissions reductions are accurate down to 100% emissions reduction (see evaluation in section A.4 of this document). However, this was not the case for 100% NO_x reduction. Consequently

two additional CMAQ/HDDM runs were performed under different levels of NOx emissions reductions. One CMAQ/HDDM run was performed with US anthropogenic NO_x cut by 50% in the 12 km Eastern domain. A second additional run was performed with a 75% NO_x reduction. Emissions of other species were not modified from the base case in these two NOx reduction runs. These addition HDDM simulations give NO_x and VOC sensitivities under expected conditions with lower NO_x emissions in the Eastern US.

Binned average diurnal sensitivity profiles were created for these two additional runs in the same manner as the sensitivity profiles were created for the base CMAQ/HDDM run. The 8-hr maximum and high/low nighttime ozone classifications were based on modeled ozone concentrations in the base run. This way, the same hours and days are included in the various bins for all three runs (and for the entire ozone adjustment process). To apply these new sensitivities a 3-step methodology was adopted. In the first step, the original base sensitivities were applied for NO_x emissions reductions less than 40%. If the desired design value was not achieved with 40% NO_x reduction then additional emissions reductions were applied using the sensitivities derived from the 50% NO_x cut simulation. For instance, to predict the effects of 60% NO_x reduction, hourly ozone concentrations were calculated for 40% NO_x emissions reductions using the base sensitivities. Then the change in ozone beyond the 40% reduction in NOx was estimated using the sensitivities from the 50% NO_x reduction simulation. Finally, the sensitivities from the 75% NO_x cut simulation were used to estimate the effects of NO_x emissions reductions beyond 75%. A conceptual picture of this process is provided in Figure 5. Equations (5)-(13) show how these calculations were performed. Note that this multi-step procedure was only performed when evaluating ozone response to NO_x emissions reductions; for estimates of ozone response to VOC emissions reductions, the base sensitivities were used over the entire range of emissions perturbations since this method is shown to accurately replicate ozone predictions from the 100% VOC cut brute force simulations (Figure 23 and Figure 24).

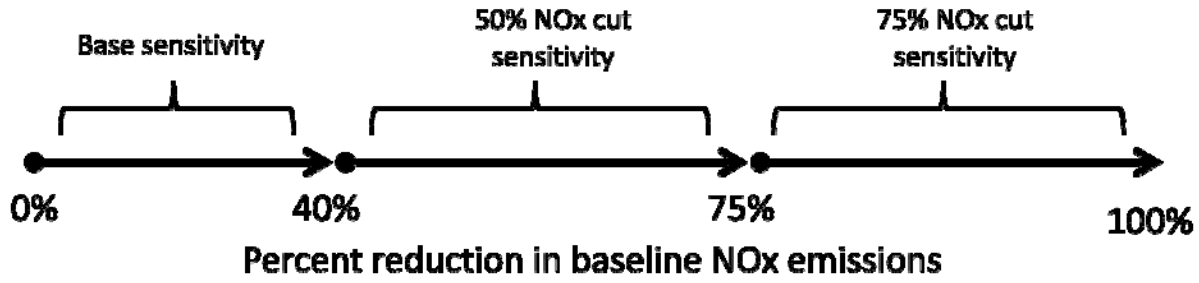

Figure 5: Conceptual picture of 3-step application of HDDM sensitivities

$$X + Y + Z = 100$$ Equation (5)

$$X = 40$$ Equation (6)

$$Y = 35$$ Equation (7)

$$z = 25$$ Equation (8)

$$P = Percent\ NOx\ reduction$$ Equation (9)

$$\Delta O_3 = \begin{cases} -a \times S_{NOx\_base} + a^2 \times S^2_{NOx\_base} & for\ P < X \\ -a \times S_{NOx\_base} + a^2 \times S^2_{NOx\_base} - b \times S_{NOx_{50}\%cut} + b^2 \times S^2_{NOx_{50}\%cut} & for\ X < P < (X+Y) \\ -a \times S_{NOx\_base} + a^2 \times S^2_{NOx\_base} - b \times S_{NOx_{50}\%cut} + b^2 \times S^2_{NOx_{50}\%cut} - c \times S_{NOx_{75}\%cut} + c^2 \times S^2_{NOx_{75}\%cut} & for\ P > (X+Y) \end{cases}$$ Equation (10)

$$a = \begin{cases} \frac{P}{100} & for\ P < X \\ \frac{X}{100} & for\ P \geq X \end{cases}$$ Equation (11)

$$b = \begin{cases} \frac{2 \times (P-X)}{100} & for\ P < Y \\ \frac{2 \times Y}{100} & for\ P \geq Y \end{cases}$$ Equation (12)

$$C = 4 \times \left(P - (X+Y)\right)$$ Equation (13)

Figure 6 demonstrates how this three-step application of HDDM sensitivities is implemented. A different version of this figure could be created for each hour, each monitoring site, and each 8-hr maximum ozone bin. The solid lines in the figure show the change in ozone concentrations (ppb) for every possible change in NO_x emissions (%). The segment of the solid line shown in black represents the portion of the NO_x reduction spectrum that uses the base sensitivity, the segment shown in blue represents the portion of the NO_x emissions reduction spectrum that uses the sensitivity from the 50% NO_x cut HDDM run, and the segment shown in green uses the sensitivity from the 75% NO_x cut HDDM run. The dotted black line shows the predicted change in ozone if the base sensitivity were used for the whole range of NO_x emissions reductions and the dotted blue line show the predicted change in ozone if only the base and 50% NO_x cut sensitivities were used. The turquoise dots represent change in ozone at 9 am for this location estimated by brute force CMAQ runs with 30%, 50%, 75%, and 100% NO_x cuts for all days in June and July 2005 that had modeled 8-hr daily maximum ozone values greater than 75 ppb.

Several features of the 3 step HDDM model-based adjustment approach are apparent from this figure. First, for this particular site/hour/bin, the base sensitivity would lead to net ozone

increases at all points in the NO_x emissions reduction spectrum, while using the sensitivities from the 50% and 75% NO_x reduction simulations lead to predictions of ozone decreases when cuts are greater than about 50%. In this case, the use of the three-step application of HDDM sensitivities leads to greater predicted ozone decreases than would be achieved with a two-step application of HDDM sensitivities. This behavior is often, but not always apparent; there are limited hours/sites/bins for which the three-step estimates lead to smaller ozone decreases than the two-step estimates would. The spread of the turquoise dots shows that there is variability in modeled ozone responses even within bins at a single site and at a single time of day. The model-based adjustment approach is supposed to predict "typical" response, but may reduce the amount of variability in model estimated ozone reductions that would be seen in brute force model runs. However, Figure 6 demonstrates that for this instance the three-step application of HDDM sensitivities does a better job of capturing an average trend in ozone response than the one- or two-step application of HDDM sensitivities. Again, this holds true in most cases but may not be the case at every site for every hour and every ozone bin. Figure 7 demonstrates the same information as Figure 6 except that it shows a nighttime hour. In Figure 7, the black, blue, and green lines (turquoise dots) are used to demonstrate estimated ozone response on a high ozone night while the red, magenta, and purple lines (pink asterisks) show response on a low ozone night. In this case, it can be seem that on high ozone nights, the 3-step HDDM application of HDDM sensitivities predicts ozone decreases in response to NO_x emissions reductions while on low ozone nights, this methodology predicts ozone increases in response to NO_x emissions reductions.

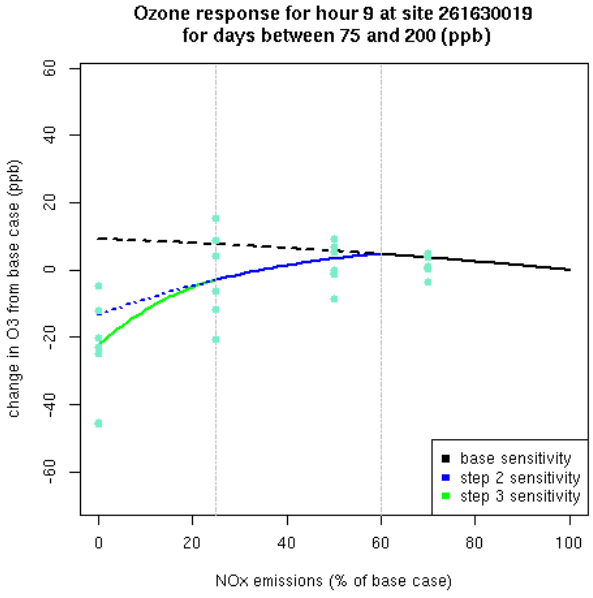

Figure 6: Example of 3 step application of HDDM sensitivities for 9am hours at Detroit site 261630019 for days with maximum daily 8-hr ozone concentrations greater than 75 ppb.

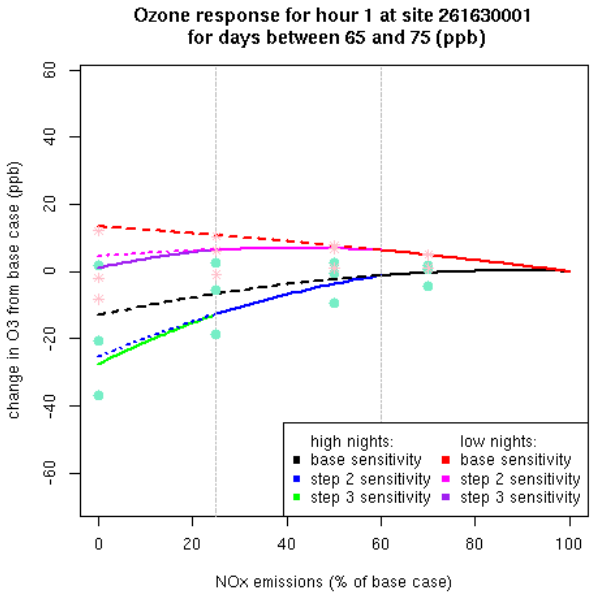

Figure 7: Example of 3 step application of HDDM sensitivities for 1am hours at Detroit site 261630001 for days with maximum daily 8-hr ozone concentrations between 65 and 75 ppb.

3.3 PROPOSED REVISIONS FOR THE SECOND DRAFT REA

Several updates to this analysis are planned for the second draft of the REA. First, EPA's Office of Air Quality Planning and Standards is currently developing a 2007-based modeling platform which includes 2007 meteorology and a combination of 2007 and 2008 emissions inputs. These more recent emissions are more relevant to this analysis which focuses on ambient data from 2006-2008. It is anticipated that this new modeling platform will be available in time for use in preparing the 2nd draft of the REA. The 2007 model run will include the entire ozone season and, thus, increase available data points for creating binned sensitivities compared to the 2005-based test cases. Second, EPA's Office of Research and Development released a newer version of the CMAQ model (v5.0) in February 2012. CMAQv5.0 is not yet instrumented with HDDM capabilities, but if this capability is available in time, we will consider using this most recent version of CMAQ. Third, we will explore other approaches for grouping modeled and observed days into bins and calculating average sensitivities. Fourth we will expand this analysis to include all 16 cities evaluated in the exposure assessment, cover ambient data from 2008-2010 and evaluate alternate possible new NAAQS in addition to the current 75 ppb standard. Finally, we will extend the analysis to include the estimation of risk and exposure based on the HDDM adjusted ozone.

4. USING HDDM/CMAQ FOR SIMULATIONS OF JUST MEETING ALTERNATIVE STANDARDS: RESULTS

4.1 ATLANTA RESULTS

4.1.1 New distributions of ozone to attain 75 ppb NAAQS

Figure 8 shows how the distribution of ozone concentrations is predicted to change by hour of day according to the model-based adjustment approach (NO_x reductions only) for a downtown site. The model-based adjustment approach predicts that ozone will respond differently at different times of day. For mid-morning and afternoon hours, adjusted ozone concentrations are lower than observed values. During evening hours, the HDDM sensitivities show very little response of ozone to NO_x cuts. Nighttime ozone concentrations are estimated to decrease due to the NO_x reductions and morning ozone concentrations (4 am-7 am) are predicted to increase due to NO_x disbenefits during the morning rush hour. This change in ozone response with time of day was not possible to replicate with quadratic rollback. Figure 9 shows the same information as Figure 8 except for a downwind monitoring location. At the downwind site, ozone decreases in the adjusted case occur at all hours and the response in the evening hours is much larger than it was for the urban site. The HDDM sensitivities are predicting different chemical regimes during rush hour for the urban and the downwind sites: the urban site is predicted to be NO_x saturated while the downwind site is not. Consequently, the urban site shows increases or lack of response during the rush hour times while the downwind site shows response of ozone to NO_x reductions at all times. Again, the quadratic rollback technique does not capture the spatial variability in ozone response within an urban area that is exhibited in the HDDM-based results.

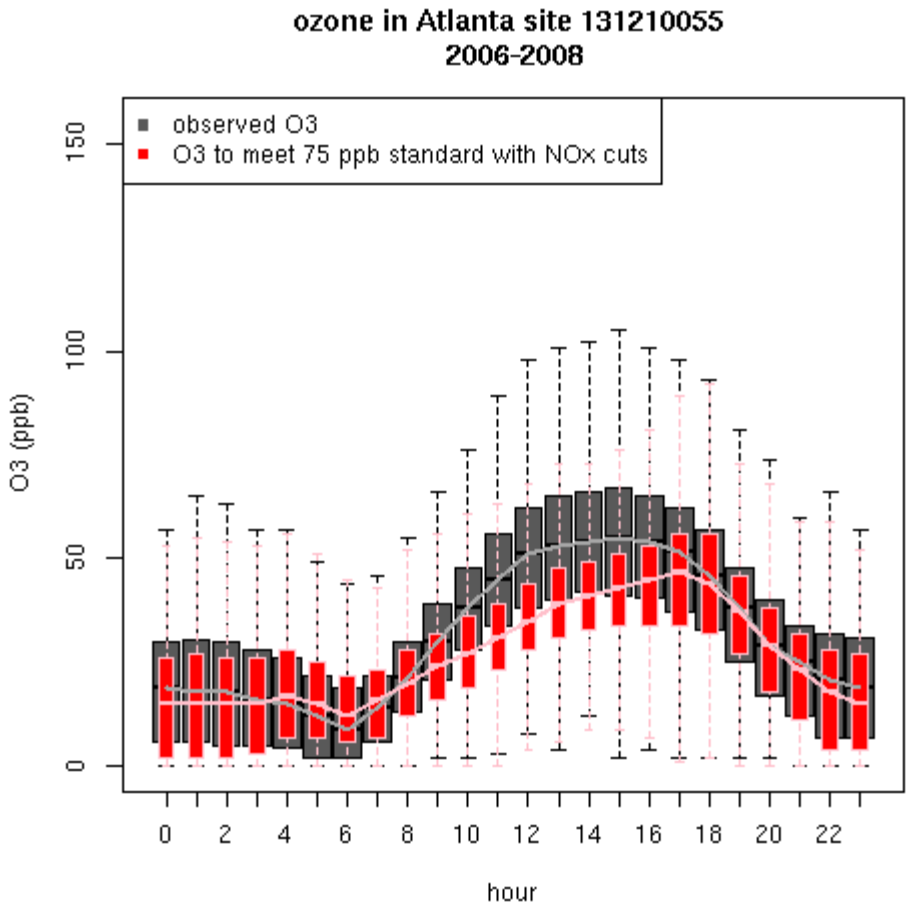

Figure 8: Distribution of ozone concentrations by hour of day for Atlanta site 131210055. Centerlines show median values, boxes designate 25th to 75th percentile values and whiskers extend to 1.5 times the interquartile range. Values in gray/black show measured ozone distributions (2006-2008) and values in red/pink show predicted ozone distributions based on HDDM model-based adjustment approach (2006-2008).

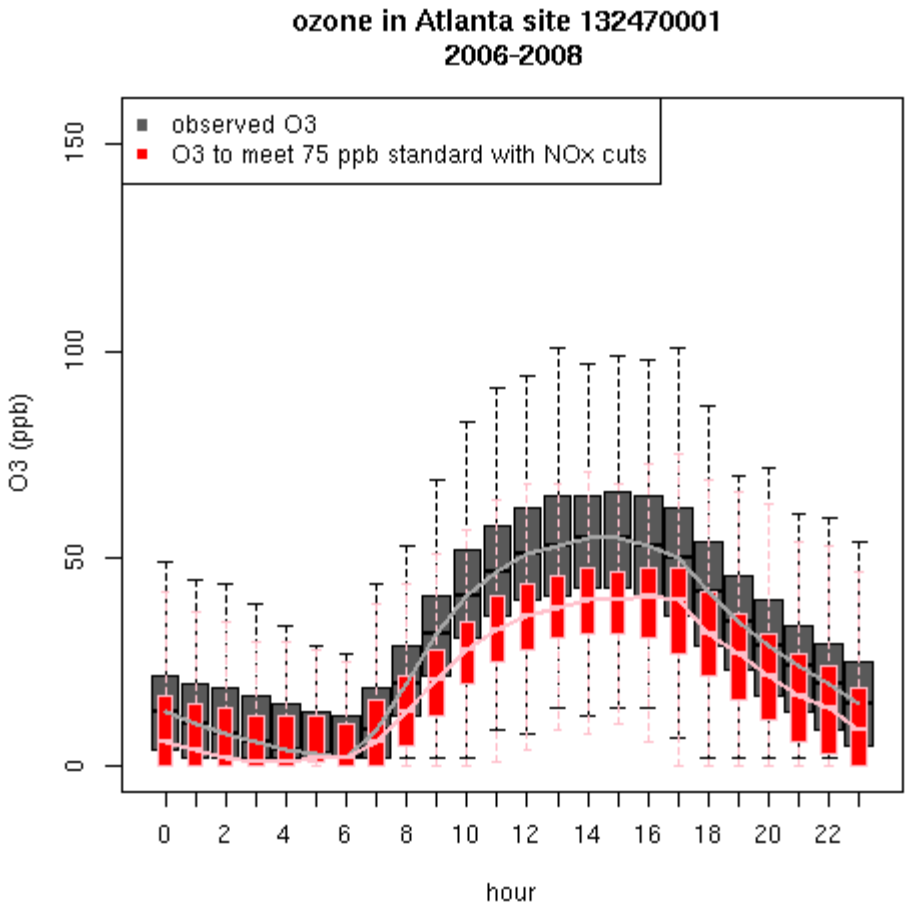

Figure 9: Distribution of ozone concentrations by hour of day for Atlanta site 132470001. Centerlines show median values, boxes designate 25th to 75th percentile values and whiskers extend to 1.5 times the interquartile range. Values in gray/black show measured ozone distributions (2006-2008) and values in red/pink show predicted ozone distributions based on HDDM model-based adjustment approach (2006-2008).

4.1.2 Resulting design values

The resulting design values for all sites in Atlanta with the model-based adjustment approach are shown in Table 1. The highest monitor in the observed data is 132470001 which is a site downwind of Atlanta. As might be expected based on the results shown in Figure 8 and Figure 9, the downwind sites show greater overall decreases in ozone with NO_x reductions than the downtown sites due to NO_x saturated conditions in the urban core during some hours of the day. Figure 7 shows that at some times smaller NO_x reductions would lead to ozone increases while larger NO_x reductions would lead to ozone decreases at some urban sites. This trend can be seen in the observed and HDDM adjusted design values. The two urban sites (131510002

and 132470001) show the smallest ozone decrease. Consequently, the model-based adjustment approach predicts that the highest design value is at the downtown site, 130890002, after the application of NOx emissions reductions. Therefore, the spatially and temporally varying sensitivities not only lead to differences in response during rush-hour times (as discussed in section 4.1.1), but also lead to difference in response of 8-hr daily maximum ozone values.

4.1.3 Comparison to quadratic rollback

Table 1 also compares predicted design values using HDDM model-based adjustment approach versus quadratic rollback. The quadratic rollback methodology requires that ozone at all sites responds the same, so unlike the HDDM approach, the quadratic rollback predicts that the relative order of high to low design value sites remains constant. Design values at the two downtown sites are lower in the quadratic rollback case while design values at all other sites are lower in the model-base adjustment approach case.

Table 1: Observed, model adjusted and rolled-back design values for Atlanta sites. Urban sites highlighted in blue.

Monitor	Measured 2006-2008 DV	HDDM Adjusted DV	Quadratic Rolled-back DV
130670003	85	65	69
130770002	84	63	68
130890002	93	75	73
130970004	87	66	70
131130001	86	65	69
131210055	91	73	72
131350002	88	65	71
131510002	94	73	74
132230003	80	59	66
132470001	95	71	75

Figure 10 shows the distribution of hourly ozone concentrations at all Atlanta sites for the observed values, the model-based adjustment approach case, and the quadratic rollback case. This comparison shows that the model-based adjustment approach reduces the hourly ozone values more through most of the distribution than quadratic rollback (i.e. the 25^{th}, 50^{th}, 75^{th}, 95^{th} percentile values are lower) but that quadratic rollback reduces the highest hourly ozone value more.

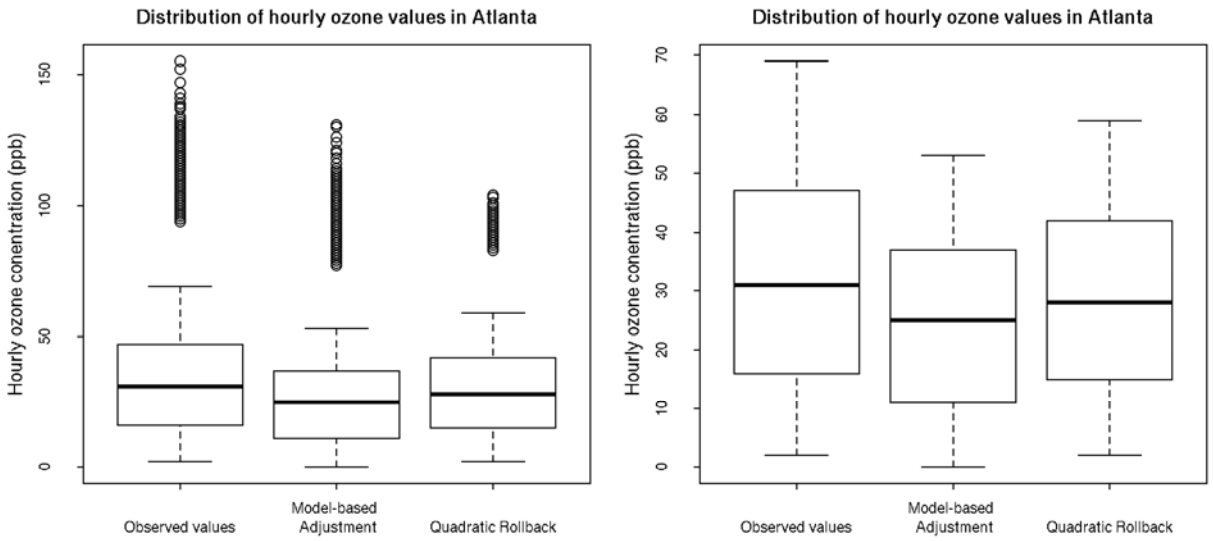

Figure 10: Distribution of ozone concentrations for all Atlanta sites (2006-2008) for measured values (left), values calculated using the model-based adjustment approach (NO_x reductions) (middle) and values calculated using quadratic rollback (right). Centerlines show median values, boxes cover 25th to 75th percentile ranges and whiskers extend to 5th and 95th percentile values. Left panel includes outlier values while right panel focuses on the portion of the range which includes the 5th to 95th percentile values.

4.2 DETROIT RESULTS

4.2.1 New distributions of ozone to attain 75 ppb NAAQS: NO_x and VOC reductions

Figure 11 and Figure 12 show ozone distributions for an urban and downwind Detroit site based on observations (2006-2008) and on the model-based adjustment approach assuming NO_x reductions. Figure 13 and Figure 14 show the same information but instead using HDDM sensitivities to VOC emissions reductions. The NO_x cut HDDM adjustment case for the Detroit urban site shows the same morning disbenefits (ozone increase) as was seen at the Atlanta downtown site. However, the response during the rest of the day looks somewhat different than the downtown Atlanta site. At the site shown in Figure 11, the high end of the ozone distribution (shown as the upper black and pink whiskers for observed and adjusted ozone) increases during the morning rush hour times (and one evening hour) but decreases at all other times of day in the model-based adjustment case. The median ozone values, however, increase throughout the day in the model-based adjustment case. This indicates that under a NO_x reduction scenario this urban Detroit site is expected to see decreases in design values but will also see increases in 8-hr daily maximum ozone on days below the standard. Note that the median observed values are quite low (less then 40 ppb) so these increases in ozone

concentrations occur on low ozone days even though they are in the middle of the observed ozone distribution for this site (i.e., this site has a larger number of low ozone days despite having a design value above 75 ppb). Figure 12 shows that at the downwind Detroit site, there are some small NO_x disbenefits in the morning and that NO_x cuts result in ozone decreases throughout the entire range of ozone for all other hours of the day. The ozone design values with VOC emissions reductions (shown in Figure 13 and Figure 14) show that ozone would be reduced at all hours of the day and for all portions of the distribution. However, the high end (top whiskers) of the ozone concentrations are not reduced as dramatically in VOC reduction for these two sites as it is with NO_x reduction. For the VOC reduction case, ozone at the urban site responds more than ozone at the downwind site.

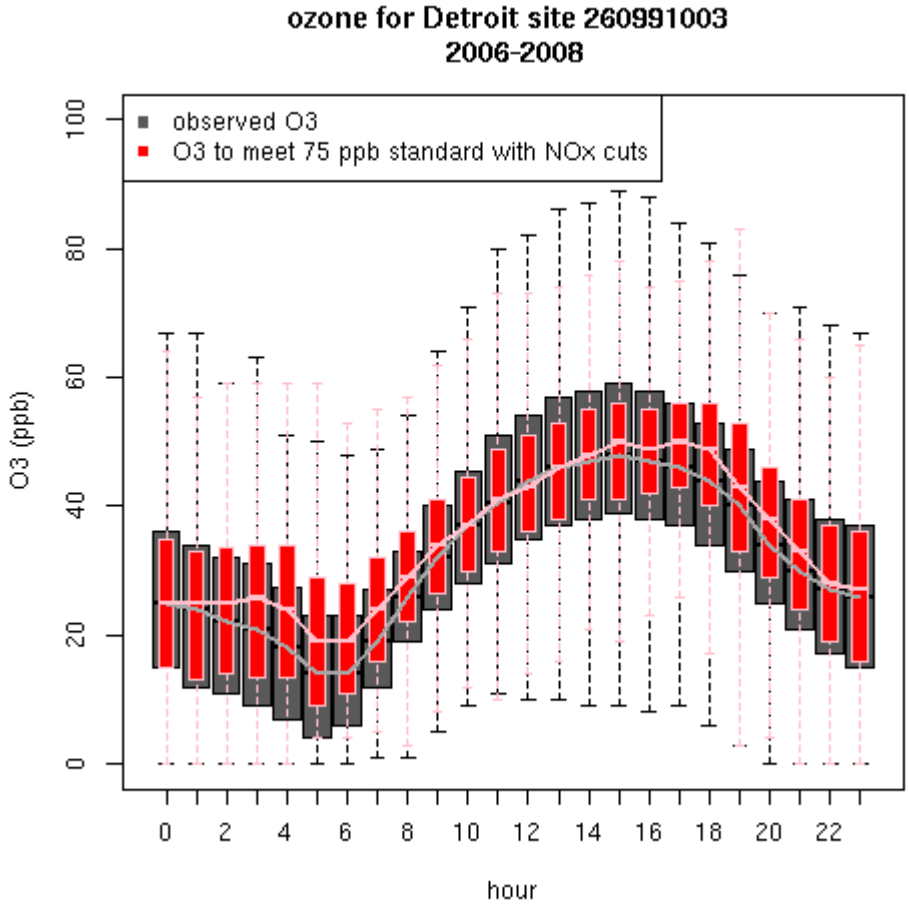

Figure 11: Distribution of ozone concentrations by hour of day for Detroit site 260991003. Centerlines show median values, boxes designate 25th to 75th percentile values and whiskers extend to 1.5 times the interquartile range. Values in gray/black show measured ozone distributions (2006-2008) and values in red/pink show predicted ozone distributions based on HDDM model-based adjustment approach (NO_x cut) (2006-2008).

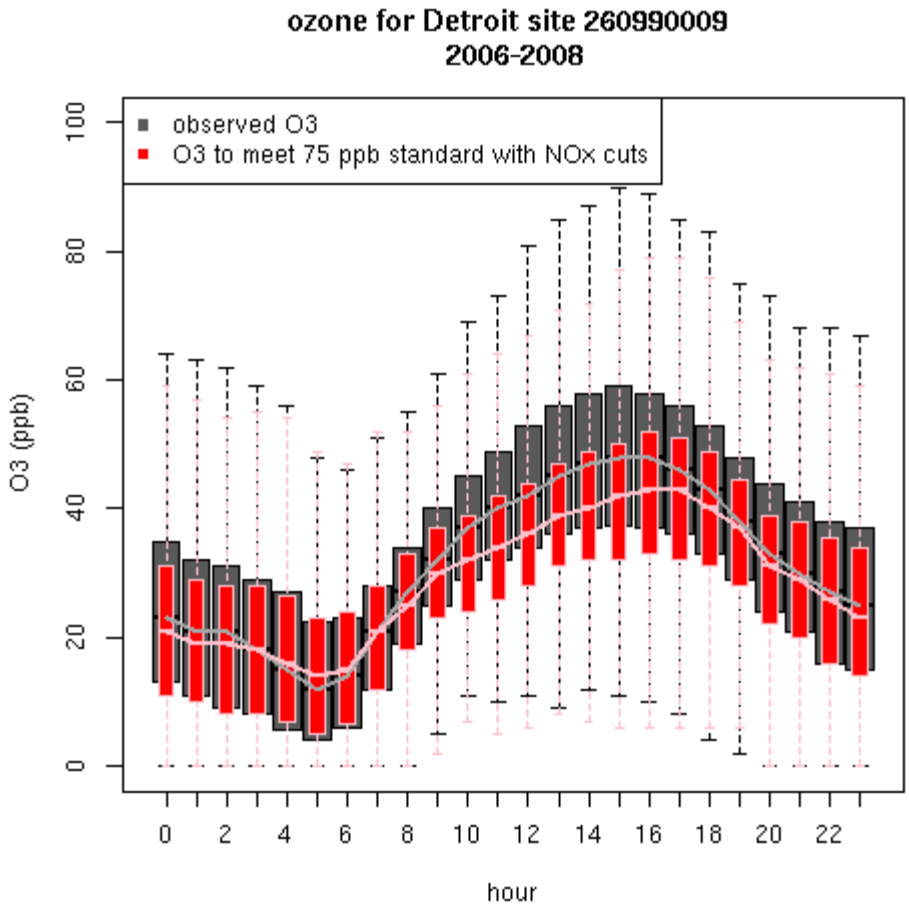

Figure 12: Distribution of ozone concentrations by hour of day for Detroit site 260990009. Centerlines show median values, boxes designate 25th to 75th percentile values and whiskers extend to 1.5 times the interquartile range. Values in gray/black show measured ozone distributions (2006-2008) and values in red/pink show predicted ozone distributions based on HDDM model-based adjustment approach (NO_x cut) (2006-2008).

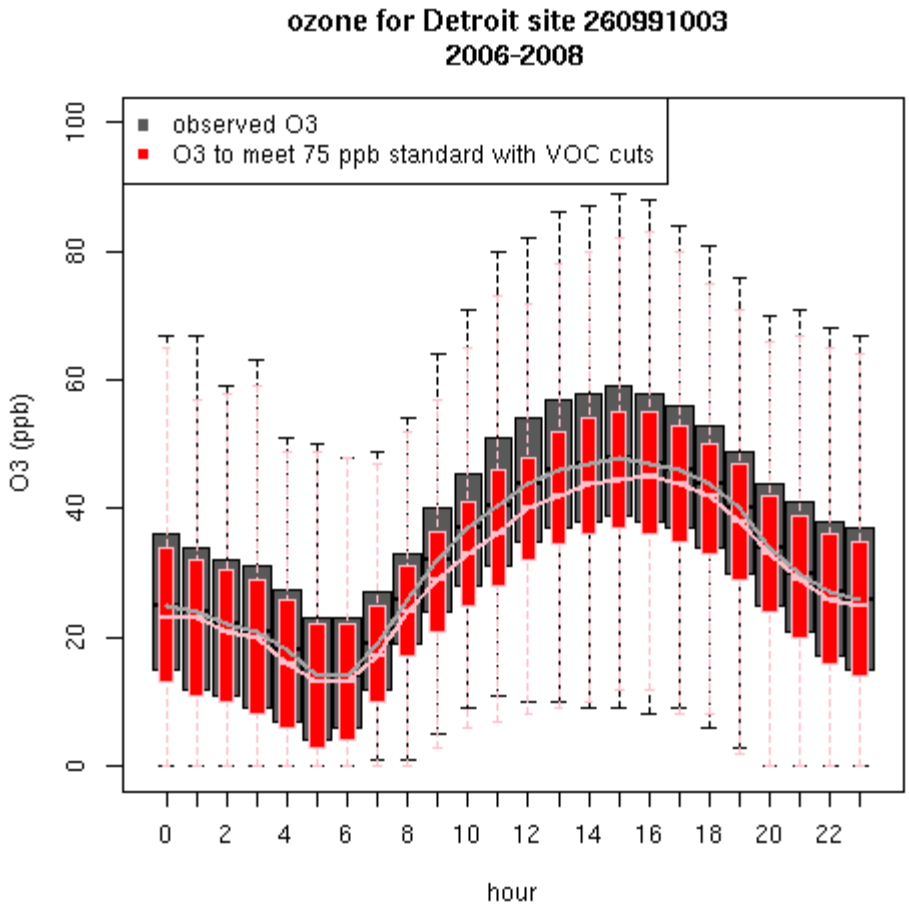

Figure 13: Distribution of ozone concentrations by hour of day for Detroit site 260991003. Centerlines show median values, boxes designate 25th to 75th percentile values and whiskers extend to 1.5 times the interquartile range. Values in gray/black show measured ozone distributions (2006-2008) and values in red/pink show predicted ozone distributions based on HDDM model-based adjustment approach (VOC cut) (2006-2008).

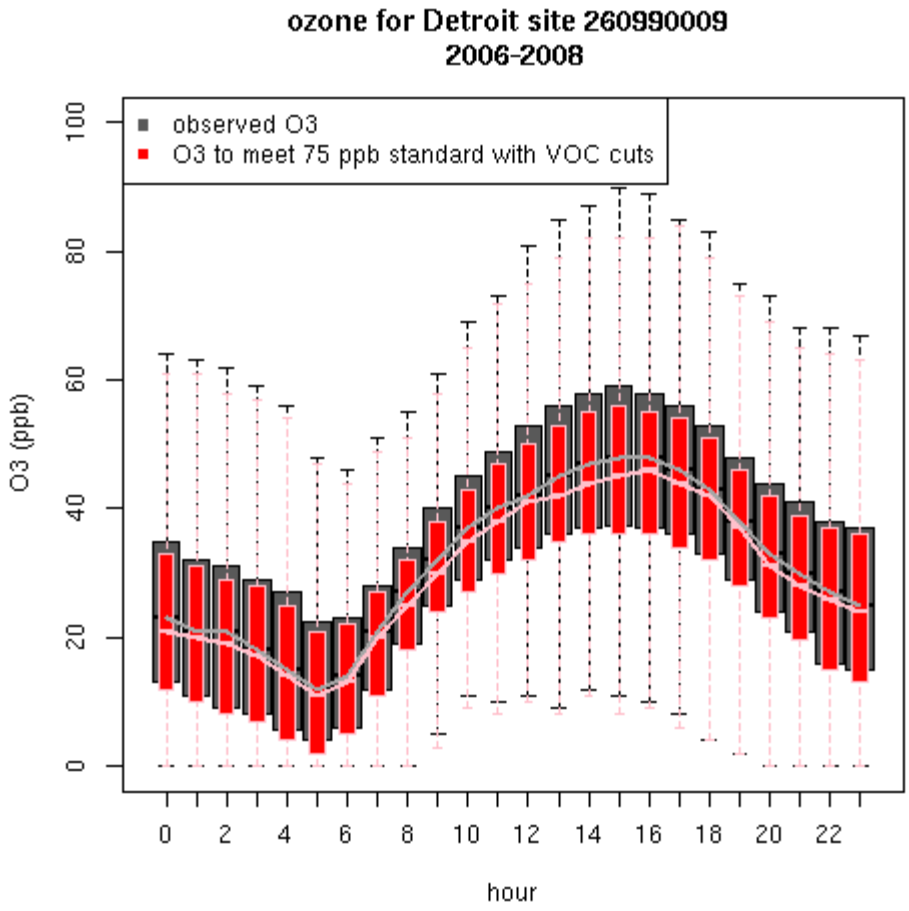

Figure 14: Distribution of ozone concentrations by hour of day for Detroit site 260990009. Centerlines show median values, boxes designate 25th to 75th percentile values and whiskers extend to 1.5 times the interquartile range. Values in gray/black show measured ozone distributions (2006-2008) and values in red/pink show predicted ozone distributions based on HDDM model-based adjustment approach (VOC cut) (2006-2008).

4.2.2 Resulting design values: NO_x and VOC reductions

Table 2 shows the resulting design values from the two adjustment scenarios for each monitor for the 75 ppb attainment case. In Detroit, there are four sites which are located in heavily urbanized areas (261630001, 261250001, 260991003, and 261630019). Ozone design values at these four sites decrease less than they do at the other less urbanized sites in Detroit for the NO_x cut case. Conversely, ozone design values decrease the same or slightly more for the urban sites than the upwind and downwind sites for the VOC reduction case. However, all but two sites are predicted to have lower design values when the 75 ppb standard is met with NO_x reductions than with VOC reductions: urban site 261630001 is predicted to have the same

design value in the NO_x and VOC model-based adjustment cases while urban site 2609910003 is predicted to have a higher design value with the NO_x reduction case than with the VOC HDDM reduction case.

4.2.3 Comparison to quadratic rollback

Table 2 also shows a comparison of both HDDM model-based adjustment cases to the predicted design values with quadratic rollback. Again, the quadratic rollback assumes that all sites will respond the same to a given level of emissions reductions so in the quadratic rollback case the order of high to low design values at Detroit sites does not change. However, in both the NO_x and VOC model-based adjustment cases some sites are more responsive than others to emissions reductions and thus the site with the highest post-control design value is different from the site with the highest measured design value for 2006-2008. Figure 15 shows the distribution of hourly ozone concentrations for all sites in Detroit from 2006-2008 based on observations, model-based adjustments (both NO_x and VOC emissions reduction cases), and quadratic rollback. Ozone distributions for quadratic rollback and model-based adjustment using VOC reductions look similar. Both show small reductions 25^{th}, 50^{th}, 75^{th} , and 95^{th} percentile values. The distribution of hourly ozone values in the NO_x reduction model-based adjustment case shows a larger decrease in the 95^{th} percentile value than the VOC model-based adjustment or quadratic rollback cases. However the NO_x reduction model-based adjustment case in Detroit leads to almost no change in the 50^{th} and 75^{th} percentile ozone values and a very small decrease in the 5^{th} and 25^{th} percentile ozone values. Therefore, in Detroit the NO_x reduction results in lowering the highest ozone concentrations more than either the VOC reduction or quadratic rollback cases but results in lowering the mid range ozone concentrations less than the VOC reduction and quadratic rollback cases.

Table 2: Observed, model adjusted, and rolled-back design values for Detroit sites. Urban sites highlighted in blue.

Monitor	Measured 2006-2008 DV	HDDM Adjusted DV (VOC reductions)	HDDM Adjusted DV (NO_x reductions)	Quadratic Rolled-back DV
261630001	71	65	65	65
261610008	74	68	65	68
260910007	75	71	63	69
261250001	77	72	70	70
261470005	78	74	67	71
260991003	80	73	75	74
260990009	81	75	72	74
261630019	82	74	71	75

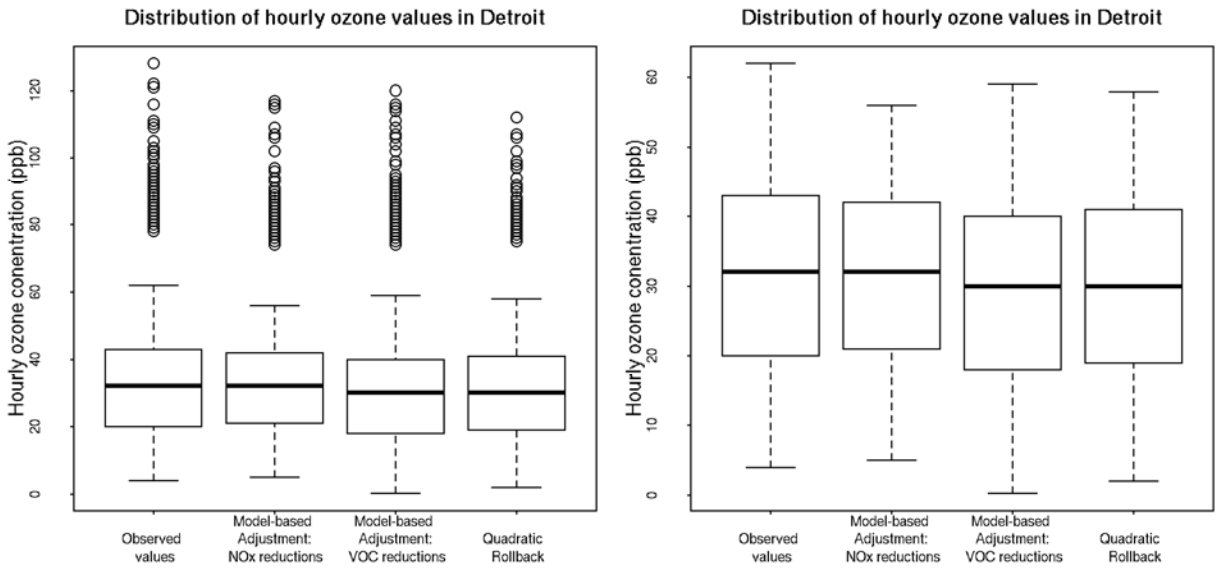

Figure 15: Distribution of ozone concentrations for all Detroit sites (2006-2008) for measured values (left), values calculated using HDDM model-based adjustment approach (NO_x reductions) (2nd from left), HDDM model-based adjustment approach (VOC reductions) (2nd from right) and values calculated using quadratic rollback (right). Centerlines show median values, boxes cover 25th to 75th percentile ranges and whiskers extend to 5th and 95th percentile values. Left panel includes outlier values while right panel focuses on the portion of the range which includes the 5th to 95th percentile values.

5. **RECOMMENDATIONS**

Based on the analysis presented here, we believe that there are clear benefits for using model-based ozone adjustments for the second draft REA. The HDDM model-based adjustment approach, unlike quadratic rollback, allows us to predict the temporally- and spatially-varying response of ozone within an urban area to emissions changes and allows us to account for the sensitivity of these air quality changes to NOx versus VOC emissions reductions. For example, the model-based adjustments account for ozone increases with NOx emissions reductions which may occur at times and locations where NOx to VOC concentration ratios are high and total ozone concentrations are low. The model-based methodology also directly accounts for physical and chemical processes that lead to ozone formation and transport, and includes both natural and anthropogenic sources of ozone precursors from sources both within and outside of the U.S. Consequently, it is more straightforward to isolate the ozone response to U.S. emission reductions, eliminating the need to artificially specify a floor for air quality changes as is required in the quadratic rollback method. The effect of these capabilities is clearly shown in this work where the order of the monitoring sites with respect to the highest to lowest ozone design values changed in both Detroit and Atlanta between the 2006-2008 observations and the HDDM model-based ozone estimates. (The application of the quadratic rollback will not change the order of the monitoring sites with respect to magnitude of the design value before versus after rollback.) Using the HDDM model-based adjustment approach also had the effect of changing the absolute predicted magnitude of the design values after simulating just meeting the current standard in the two case study areas, when compared to the application of the quadratic rollback. For example, the application of the model-based adjustments in Atlanta resulted in 8 out of 10 monitoring sites with lower design values than those estimated by using quadratic rollback. In the Detroit case study example, the application of HDDM allowed us to compare the effect of reducing NOx versus VOC emissions. Five out of 8 monitoring sites in Detroit were predicted to have lower design values using the HDDM model-based adjustment approach with NOx emissions reductions versus quadratic rollback but only 2 out of 8 sites were predicted to have lower design values using HDDM model-based adjustment approach with VOC emissions reductions versus quadratic rollback. Compared to quadratic rollback, these capabilities of the HDDM model-based adjustment approach build confidence that the results drawn from this type of analysis allow us to more realistically represent the response in hourly ozone concentrations to reductions in emissions for a scenario of just meeting the current and alternative standard levels. Further analyses will be conducted to better understand the effect of using the HDDM model-based adjustment approach on the results of the risk and exposure assessment.

6. **REFERENCES**

Appel, K.W., Gilliland, A.B., Sarwar, G., Gilliam, R.C. (2007). Evaluation of the Community Multiscale Air Quality(CMAQ) model version 4.5: Sensitivities impacting model performance Part I - Ozone. Atmospheric Environment, 41: 9603-9615.

Appel, K.W., Bhave, P.V., Gilliland, A.B., Sarwar, G., Roselle, S.J. (2008). Evaluation of the community Multiscale air quality (CMAQ) model version 4.5: Sensitivities impacting model performance; Part II - particulate matter. Atmospheric Environment, 42: 6057-6066.

Baker, K. and P. Dolwick. Meteorological Modeling Performance Evaluation for the Annual 2005 Eastern U.S. 12-km Domain Simulation, USEPA/OAQPS, February 2, 2009.

Baker, K. and P. Dolwick. Meteorological Modeling Performance Evaluation for the Annual 2005 Western U.S. 12-km Domain Simulation, USEPA/OAQPS, February 2, 2009.

Baker, K. and P. Dolwick. Meteorological Modeling Performance Evaluation for the Annual 2005 Continental U.S. 36-km Domain Simulation, USEPA/OAQPS, February 2, 2009.

Byun, D.W., and Ching, J.K.S., Eds, 1999. Science algorithms of EPA Models-3 Community Multiscale Air Quality (CMAQ modeling system, EPA/600/R-99/030, Office of Research and Development).

Byun, D., Schere, K.L. (2006). Review of the governing equations, computational algorithms, and other components of the models-3 Community Multiscale Air Quality (CMAQ) modeling system. Applied Mechanics Reviews, 59: 51-77.

Carlton, A.G., Bhave, P.V., Napelenok, S.L., Edney, E.D., Sarwar, G., Pinder, R.W., Pouliot, G.A., Houyoux, M. (2010). Model Representation of Secondary Organic Aerosol in CMAQv4.7. Environmental Science & Technology, 44: 8553-8560.

Cohan, D.S., Hakami, A., Hu, Y., Russell, A.G. (2005). Nonlinear response of ozone to emissions: Source apportionment and sensitivity analysis. Environmental Science & Technology, 39: 6739-6748.

Cohan, D.S., Napelenok, S.L. (2011). Air quality response modeling for decision support. Atmosphere, 2: 407-425; doi:10.3390/atmos2030407.

Dunker, A.M. (1984). The decoupled direct method for calculating sensitivity coefficients in chemical kinetics. Journal of Chemical Physics, 81; 2385-2393.

Foley, K.M., Roselle, S.J., Appel, K.W., Bhave, P.V., Pleim, J.E., Otte, T.L., Mathur, R., Sarwar, G., Young, J.O., Gilliam, R.C., Nolte, C.G., Kelly, J.T., Gilliland, A.B., Bash, J.O. (2010). Incremental testing of the Community Multiscale Air Quality (CMAQ) modeling system version 4.7, Geoscientific Model Development, 3: 205-226.

Grell, G., J. Dudhia, and D. Stauffer (1994). A Description of the Fifth-Generation Penn State/NCAR Mesoscale Model (MM5), NCAR/TN-398+STR., 138 pp, National Center for Atmospheric Research, Boulder CO.

Gery, M.W., Whitten, G.Z., Killus, J.P., Dodge, M.C. (1989). A photochemical kinetics mechanism for urban and regional scale computer modeling. Journal of Geophysical Research-Atmospheres, 94: 12925-12956.

Hakami, A., Odman, M.T., Russell, A.G. (2003). High-order direct sensitivity analysis of multidimensional air quality models. Environmental Science & Technology, 37: 2442-2452.

Hakami, A., Odman, M.T., Russell, A.G. (2004). Nonlinearity in atmospheric response: A direct sensitivity analysis approach. Journal of Geophysical Research, 109: D15303; doi:10.1029/2003JD004502.

Henze, D.K., J.H. Seinfeld, N.L. Ng, J.H. Kroll, T-M. Fu, D.J. Jacob, C.L. Heald (2008). Global modeling of secondary organic aerosol formation from aromatic hydrocarbons: High-vs.low-yield pathways. Atmos. Chem. Phys., 8: 2405-2420.

Houyoux, M.R., Vukovich, J.M., Coats, C.J., Wheeler, N.J.M., Kasibhatla, P.S. (2000). Emission inventorydevelopment and processing for the Seasonal Model for Regional Air Quality (SMRAQ) project. Journal of Geophysical Research-Atmospheres, 105: 9079-9090.

Koo, B., Dunker, A.M., Yarwood, G. (2007). Implementing the decoupled direct method for sensitivity analysis in a particulate matter air quality model. Environmental Science & Technology, 41: 2847-2854.

Napelenok, S.L., Cohan, D.S., Hu, Y., Russell, A.G. (2006). Decoupled direct 3D sensitivity analysis for particulate matter (DDM-3D/PM). Atmospheric Environment, 40: 6112-6121.

National Research Council of the National Academies (2008). Estimating Mortality Risk Reduction and Economic Benefits from Controlling Ozone Air Pollution. The National Academies Press, Washington, D.C

Nenes, A., Pandis, S.N., Pilinis, C. (1998). ISORROPIA: A new thermodynamic equilibrium model for multiphasemulticomponent inorganic aerosols. Aquatic Geochemistry, 4: 123-152.

Pierce, T.; Geron, C.; Bender, L.; Dennis, R.; Tonnesen, G. Guenther, A. (1998). Influence of increased isoprene emissions on regional ozone modeling. J. Geophys. Res., 103: 25611–25629.

Seinfeld, J.H. and S.N. Pandis. (1998). Atmospheric chemistry and physics from air pollution to climate change. John Wiley & Sons, Inc, New York, 1998.

US EPA, 2007. Guidance on the Use of Models and Other Analyses for Demonstrating Attainment of Air Quality Goals for Ozone, PM2.5, and Regional Haze, Research Triangle Park. EPA-454/B-07-002: http://www.epa.gov/ttn/scram/guidance/guide/final-03-pm-rh-guidance.pdf.

US EPA, Emissions Modeling for the Final Mercury and Air Toxics Standards Technical Support Document, 2011a, EPA-45A/R-11-011: http://epa.gov/ttn/chief/emch/toxics/MATS_Final_Emissions_Modeling_TSD_9Dec2011.pdf.

US EPA, Air Quality Modeling Technical Support Document: Final EGU NESHAP, 2011b, EPA-45A/R-11-009.

US EPA, Health Risk and Exposure Assessment for Ozone: First External Review Draft, 2012, EPA 452/P-12-001.

Yang, Y.-J., Wilkinson, J.G., Russell, A.G. (1997). Fast, direct sensitivity analysis of multidimensional photochemical models. Environmental Science & Technology, 31: 2859-2868.

Yantosca, B. (2004). GEOS-CHEMv7-01-02 User's Guide, Atmospheric Chemistry Modeling Group, Harvard University, Cambridge, MA, October 15, 2004.

Yarwood, G., Rao, S., Yocke, M., Whitten, G.Z. (2005). Updates to the Carbon Bond chemical mechanism: CB05. Final Report to the US EPA, RT-0400675, December 8, 2005: http://www.camx.com/publ/pdfs/CB05_Final_Report_120805.pdf.

Zhang, W., Capps, S.L., Hu, Y., Nenes, A., Napelenok, S.L., Russell, A.G. (2012). Development of the high-order decoupled direct method in three dimensions for particulate matter: Enabling advanced sensitivity analysis in air quality models. Geoscientific Model Development, 5: 355-368.

APPENDIX A. MODEL SET-UP AND EVALUATION ANALYSES

A.1. MODEL SET-UP AND SIMULATION

The air quality modeling underlying this analysis was performed using CMAQv4.7.1 with HDDM for ozone (www.cmaq-model.org). CMAQ was run using the carbon bond 2005 (CB05) gas-phase chemical mechanism (Grey et al 1989; Yarwood et al, 2005) and the AERO5 aerosol module which includes ISORROPIA for gas-particle partitioning of inorganic species (Nenes et al 1998) and secondary organic aerosol treatment as described in Carlton et al (2010).

A.1.1. Model domain

For this analysis, all CMAQ/HDDM runs were performed in the Eastern U.S. 12 km modeling domain. As shown in Figure 16, this domain has a "parent" domain with a horizontal grid of resolution of 36 km. The air quality predictions from the 36 km domain were only used to establish the incoming air quality concentrations along the boundaries of the 12 km domain. Air quality conditions at the outer boundary of the 36 km domain were taken from a global model. For both domains, the model extends vertically from the surface to 100 millibars (approximately 15 km) using a sigma-pressure coordinate system. Table 3 provides some basic geographic information regarding the CMAQ domains.

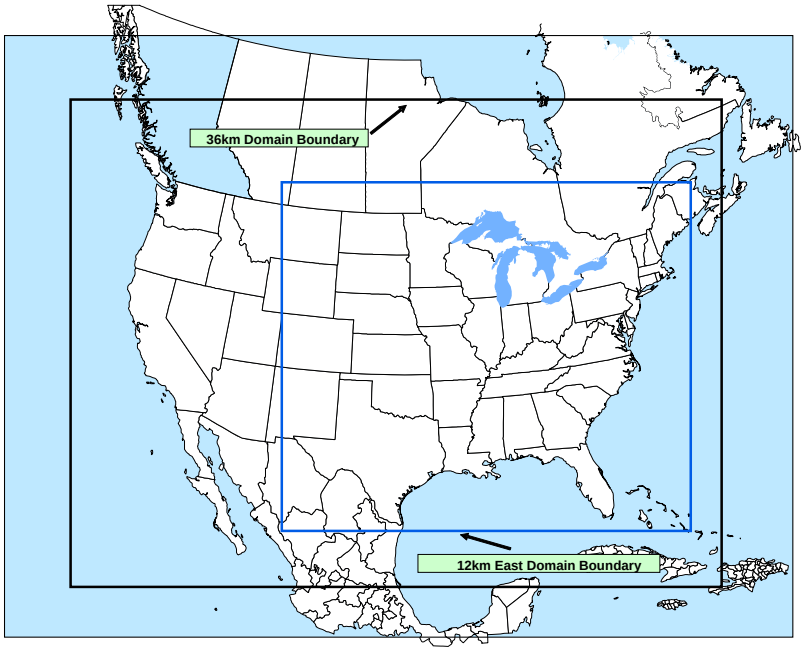

Figure 16: Map of the CMAQ modeling domain. The black outer box denotes the 36 km national modeling domain and the blue inner box is the 12 km eastern U.S. fine grid.

Table 3: Geographic elements of domain used in the CMAQ/HDDM modeling

	CMAQ Modeling Configuration	
	National Grid	**Eastern U.S. Fine Grid**
Map Projection	Lambert Conformal Projection	
Grid Resolution	36 km	12 km
Coordinate Center	97 deg W, 40 deg N	
True Latitudes	33 deg N and 45 deg N	
Dimensions	148 x 112 x 14	279 x 240 x 14
Vertical extent	14 Layers: Surface to 100 millibar level (see Table II-3)	

A.1.2. Model time period

The CMAQ/HDDM modeling domain was simulated for July and August of 2005. The simulation included at 3 day "ramp-up" period from June 28-June 30 to minimize the effects of initial conditions. The ramp-up days were not considered in the analysis for the HDDM results. Only 3 days were deemed necessary for the ramp up because the initial concentrations are derived from the 36 km parent simulation.

A.1.3. Model Inputs: meteorology, emissions, initial and boundary conditions

CMAQ model simulations require inputs of meteorological fields, emissions, and initial and boundary conditions. The gridded meteorological input data for the entire year of 2005 were derived from simulations of the Pennsylvania State University / National Center for Atmospheric Research Mesoscale Model. This model, commonly referred to as MM5, is a limited-area, nonhydrostatic, terrain-following system that solves for the full set of physical and thermodynamic equations which govern atmospheric motions (Grell et al., 1994). Meteorological model input fields were prepared separately for each of the two domains shown in Figure 16 using MM5 version 3.7.4. The MM5 simulations were run on the same map projection as CMAQ.

The 36 km and 12 km meteorological model runs configured similarly. The selections for key MM5 physics options are shown below:

- Pleim-Xiu PBL and land surface schemes
- Kain-Fritsh 2 cumulus parameterization
- Reisner 2 mixed phase moisture scheme
- RRTM longwave radiation scheme
- Dudhia shortwave radiation scheme

Three dimensional analysis nudging for temperature and moisture was applied above the boundary layer only. Analysis nudging for the wind field was applied above and below the boundary layer. The 36 km domain nudging weighting factors were 3.0×10^4 for wind fields and temperatures and 1.0×10^5 for moisture fields. The 12 km domain nudging weighting factors were 1.0×10^4 for wind fields and temperatures and 1.0×10^5 for moisture fields.

The 36 km and 12 km domain model runs were conducted in 5.5 day segments with 12 hours of overlap for spin-up purposes. Both meteorological modeling domains contained 34 vertical layers with an approximately 38 m deep surface layer and a 100 millibar top. The MM5 and CMAQ vertical structures are shown in Table 4 and do not vary by horizontal grid resolution.

Table 4: Vertical layer structure for MM5 and CMAQ (heights are layer top)

CMAQ Layers	MM5 Layers	Sigma P	Approximate Height (m)	Approximate Pressure (mb)
0	0	1.000	0	1000
1	1	0.995	38	995
2	2	0.990	77	991
	3	0.985	115	987
3	4	0.980	154	982
	5	0.970	232	973
4	6	0.960	310	964
	7	0.950	389	955
5	8	0.940	469	946
	9	0.930	550	937
	10	0.920	631	928
6	11	0.910	712	919
	12	0.900	794	910
	13	0.880	961	892
7	14	0.860	1,130	874
	15	0.840	1,303	856
	16	0.820	1,478	838
8	17	0.800	1,657	820
	18	0.770	1,930	793
9	19	0.740	2,212	766
	20	0.700	2,600	730
10	21	0.650	3,108	685
	22	0.600	3,644	640
11	23	0.550	4,212	595
	24	0.500	4,816	550
	25	0.450	5,461	505
12	26	0.400	6,153	460
	27	0.350	6,903	415
	28	0.300	7,720	370
	29	0.250	8,621	325
13	30	0.200	9,625	280
	31	0.150	10,764	235
	32	0.100	12,085	190
	33	0.050	13,670	145
14	34	0.000	15,674	100

The 2005 meteorological outputs from all three MM5 runs were processed to create model-ready inputs for CMAQ using the Meteorology-Chemistry Interface Processor (MCIP), version 3.4 (Byun and Ching, 1999).

Before initiating the air quality simulations, it is important to identify the biases and errors associated with the meteorological modeling inputs. The 2005 MM5 model performance evaluations used an approach which included a combination of qualitative and quantitative analyses to assess the adequacy of the MM5 simulated fields. Qualitative evaluations compared spatial patterns of monthly total rainfall and monthly maximum modeled planetary boundary layer (PBL) heights. The operational evaluation included statistical comparisons of model/observed pairs (e.g., mean normalized bias, mean normalized error, root mean square errors, etc.) for multiple meteorological parameters. For this portion of the evaluation, five meteorological parameters were investigated: temperature, humidity, shortwave downward radiation, wind speed, and wind direction. The MM5 evaluations for each domain are described elsewhere (Baker and Dolwick, 2005a,b,c). The results of these analyses indicate that the bias and error values associated with all three sets of 2005 meteorological data were generally within the range of past meteorological modeling results that have been used for air quality applications.

The emissions data used are based on the 2005 v4.3 platform. Emissions are processed to photochemical model inputs with the SMOKE emissions modeling system (Houyoux et al., 2000). This platform includes emissions from electric generating utilities (EGUs) and fires in the United States which are temporalized based on average temporal profiles from 3 years of data. In addition, US emissions are included from other point sources, area sources, agricultural sources (ammonia only), anthropogenic fugitive dust sources, nonroad mobile sources, onroad mobile sources, and biogenic sources. Onroad mobile sources were created using EPA's MOVES model (www.epa.gov/otaq/models/moves). Biogenic emissions were estimated using the Biogenic Emissions Inventory System version 3.14 (BEISv3.14) (Pierce et al, 1998). Other North American emissions are based on a 2006 Canadian inventory and 1999 Mexican inventory. Emissions totals within the 12 km Eastern domain are summarized in Table 5 for CO, NH_3, NO_x, PM_{10}, $PM_{2.5}$, SO_2, VOC. More details on the emission used for this modeling can be found in US EPA (2011a).

Table 5: Summary of emissions totals by sector for the 12km Eastern US domain

Sector Name	Sector description	Emissions (1000 tons/year)						
		CO	NH_3	NO_X	PM_{10}	$PM_{2.5}$	SO_2	VOC
afdust	Anthropogenic fugitive dust				7,916	924		
ag	Agricultural sources		2,874					
alm_no_c3	Air, locomotive, and marine mobile sources (except C3 marine)	224	1	1,614	49	47	110	56
avefire	Average year fire emissions	4,664	19	103	417	357	25	1,068
nonpt	Area sources	6,124	109	1,460	1,082	871	1,095	6,350
nonroad	Off road equipment	16,766	2	1,679	175	167	176	2,318
onroad	Onroad mobile vehicles	34,793	117	6,866	307	251	151	2,715
othar	Canada and Mexico area sources	2,552	411	476	783	236	104	997
othon	Canada and Mexico onroad mobile sources	3,249	16	375	12	9	7	237
othpt	Canada and Mexico point sources	634	12	537	108	84	1,161	214
ptipm	Point sources: electric generation units	567	20	3,419	570	472	10,171	38
ptnonipm	Point sources other than electric generating units	2,802	143	1,979	555	378	1,891	1,166
seca_c3	C3 marine vessels	48		578	48	44	371	20
beis	Biogenic emissions	5,401		1,644				26,555
total US anthro	Total US anthropogenic emissions used in HDDM (NOx and VOC only)			17,595				12,662
total	Domainwide total	77,822	3,723	20,729	12,021	3,840	15,264	41,734

The lateral boundary and initial species concentrations for the 36 km domain are provided by a three-dimensional global atmospheric chemistry model, the GEOS-CHEM (Yantosca, 2004) model (standard version 7-04-11(Henze et al, 2008)). The global GEOS-CHEM model simulates atmospheric chemical and physical processes driven by assimilated meteorological observations from the NASA's Goddard Earth Observing System (GEOS). This model was run for 2005 with a grid resolution of 2.0 degree x 2.5 degree (latitude-longitude) and 30 vertical layers up to 100 mb. The predictions were used to provide one-way dynamic boundary conditions at three-hour intervals and an initial concentration field for the 36 km CMAQ simulations. The outputs from the 36 km modeling were used to develop the initial/boundary concentrations for the subsequent 12 km Eastern domain model simulation.

A.2. OPERATIONAL EVALUATION OF MODELED OZONE CONCENTRATIONS IN ATLANTA AND DETROIT

An overall model performance evaluation for ozone and $PM_{2.5}$ predictions from the Eastern 12 km domain can be found in US EPA (2011b). Model evaluation statistics for specific monitors included in this analysis are provided in this section.

Table 6 and Table 7 give performance statistics for modeled ozone versus measured ozone at the Atlanta and Detroit monitoring sites respectively. Performance statistics are given both for hourly ozone (all hours of the day) and 8-hr daily maximum ozone. Aggregate statistics are given for both metrics. In addition, data are further disaggregated to show performance when observed hourly ozone or observed 8-hr daily maximum ozone is above a threshold of 60 ppb. Time series of measured and modeled hourly values in Atlanta are shown in Figure 17 and Figure 18, while a time series of 8-hr daily maximum ozone values is shown in Figure 19. The time series for Detroit are shown in Figure 20, Figure 21, and Figure 22. These tables and figures show that ozone is overpredicted at Atlanta monitoring sites during July and August 2005. This overprediction occurs both during daytime peak hours and at night. The 8-hr daily max ozone is also overpredicted in Atlanta (Figure 19), however the model shows skill in capturing the day-to-day fluctuations in ozone levels. This model overprediction makes the binning process especially important since it matches similar modeled and measured days instead of relying on perfect model performance. For sites in Detroit the predictions are more closely aligned with the observations than in Atlanta. For the most part, daytime ozone values are well captured in Detroit. The model still slightly overpredicts low nighttime ozone concentrations in Detroit, but not nearly to the extent seen in Atlanta. Although daytime ozone predictions are fairly accurate in Detroit, the binning methodology still prevents the application of sensitivities derived from high modeled ozone days to low observed ozone days and vice versa since there are still some overpredicted and some underpredicted daytime ozone values.

Table 6: Performance statistics of modeled ozone at 10 Atlanta monitoring sites used in this analysis

Metric	Hourly ozone		8-hr daily maximum ozone	
	All values	➢ 60 ppb	All values	➢ 60 ppb
Number	14,560	1533	606	166
Mean Obs (ppb)	27.0	72.5	49.2	71.3
Mean Mod (ppb)	45.1	79.7	64.1	81.2
Mean Bias (ppb)	18.0	7.2	14.9	9.9
Mean Error (ppb)	19.3	13.3	15.9	12.9
Normalized mean bias (%)	66.6	9.9	30.4	13.9
Normalized mean error (%)	71.5	18.3	32.3	18.1

Table 7: Performance statistics of modeled ozone at 8 Detroit monitoring sites used in this analysis

Metric	Hourly ozone		8-hr daily maximum ozone	
	All values	➢ 60 ppb	All values	➢ 60 ppb
Number	11,329	1362	295	88
Mean Obs (ppb)	33.6	71	53.7	71.7
Mean Mod (ppb)	37.9	63.2	55.9	67.7
Mean Bias (ppb)	4.4	-7.8	2.2	-4.1
Mean Error (ppb)	11.2	11.7	7.8	7.7
Normalized mean bias (%)	13.0	-10.9	4.1	-5.7
Normalized mean error (%)	33.4	16.6	14.5	10.7

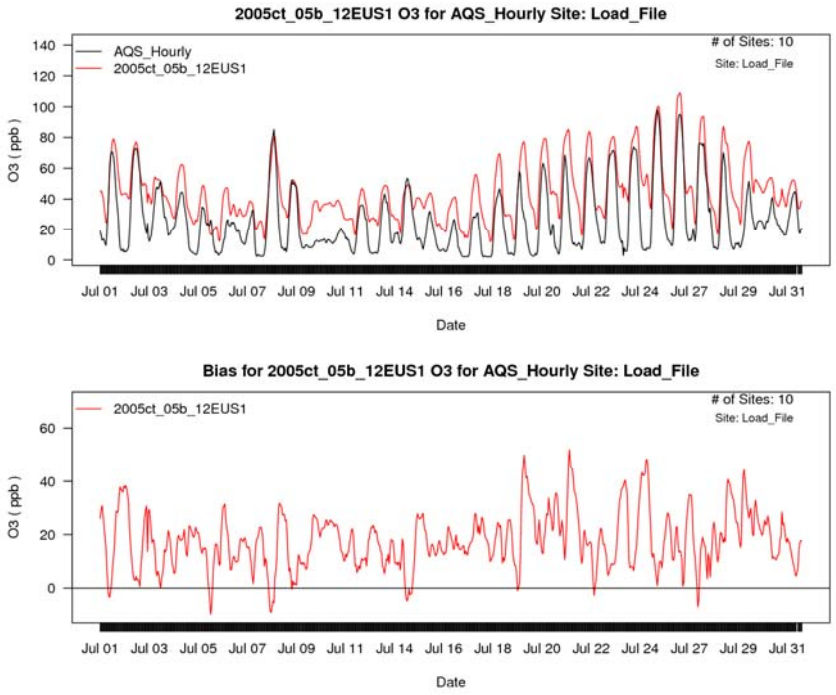

Figure 17: Time series of model performance for hourly ozone concentrations at Atlanta monitoring sites for July 2005. Observed values shown in black and modeled values shown in red.

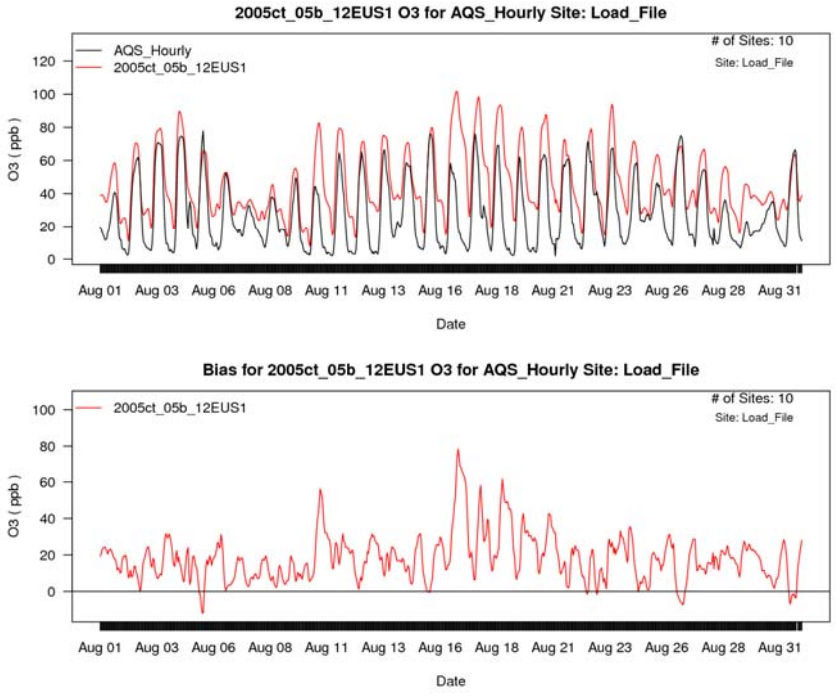

Figure 18: Time series of model performance for hourly ozone concentrations at Atlanta monitoring sites for August 2005. Observed values shown in black and modeled values shown in red.

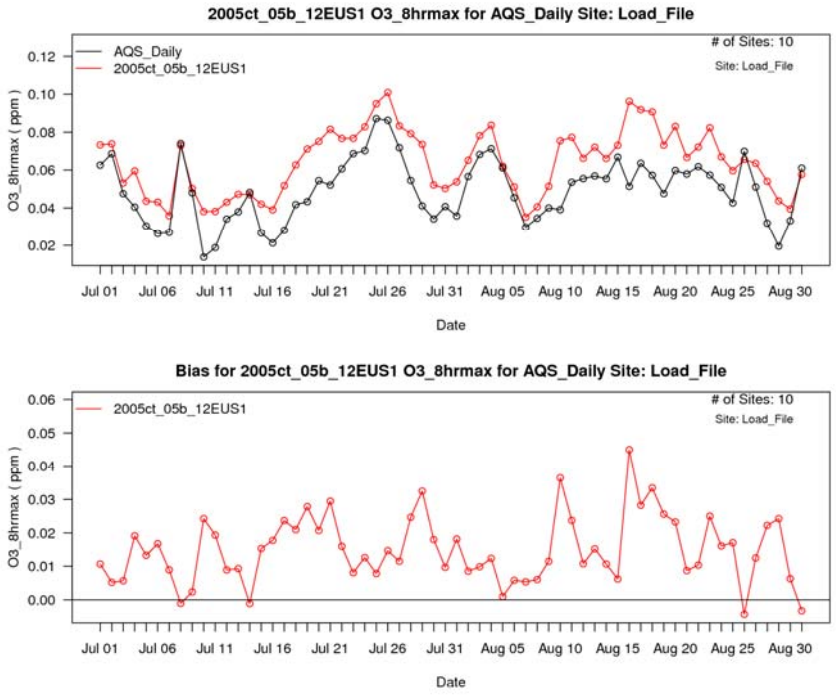

Figure 19: Time series of model performance for 8-hr daily maximum ozone concentrations at Atlanta monitoring sites for July and August 2005. Observed values shown in black and modeled values shown in red.

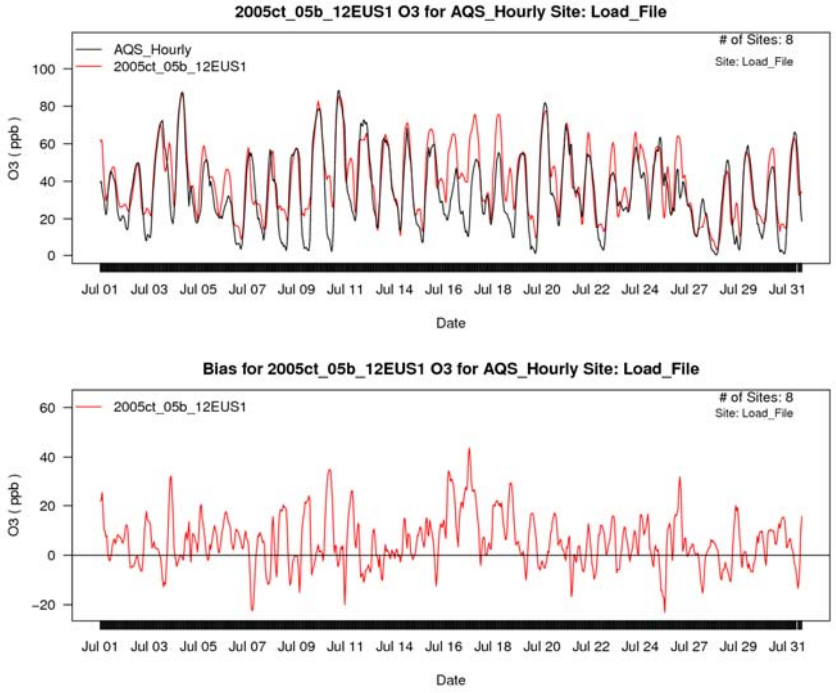

Figure 20: Time series of model performance for hourly ozone concentrations at Detroit monitoring sites for July 2005. Observed values shown in black and modeled values shown in red.

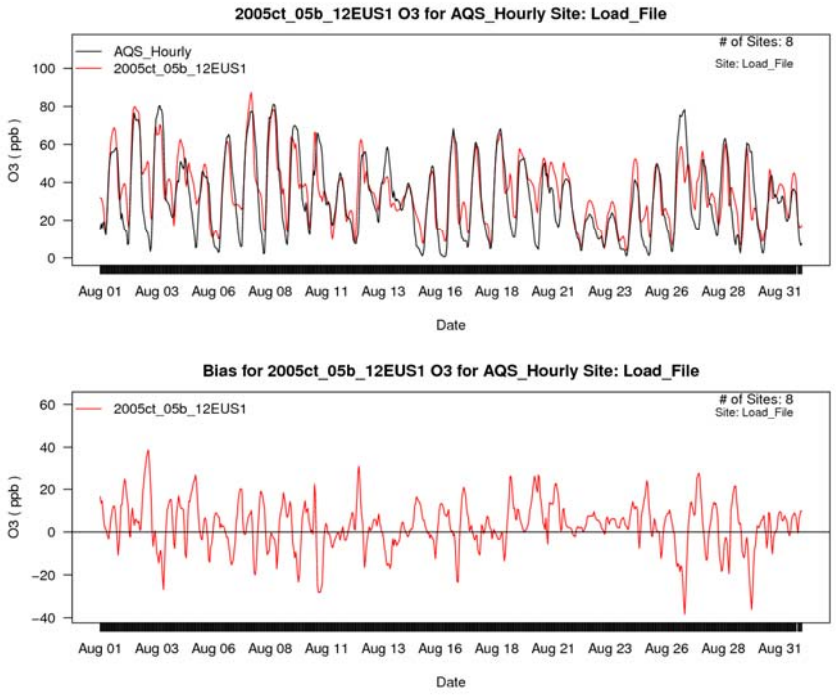

Figure 21: Time series of model performance for hourly ozone concentrations at Detroit monitoring sites for August 2005. Observed values shown in black and modeled values shown in red.

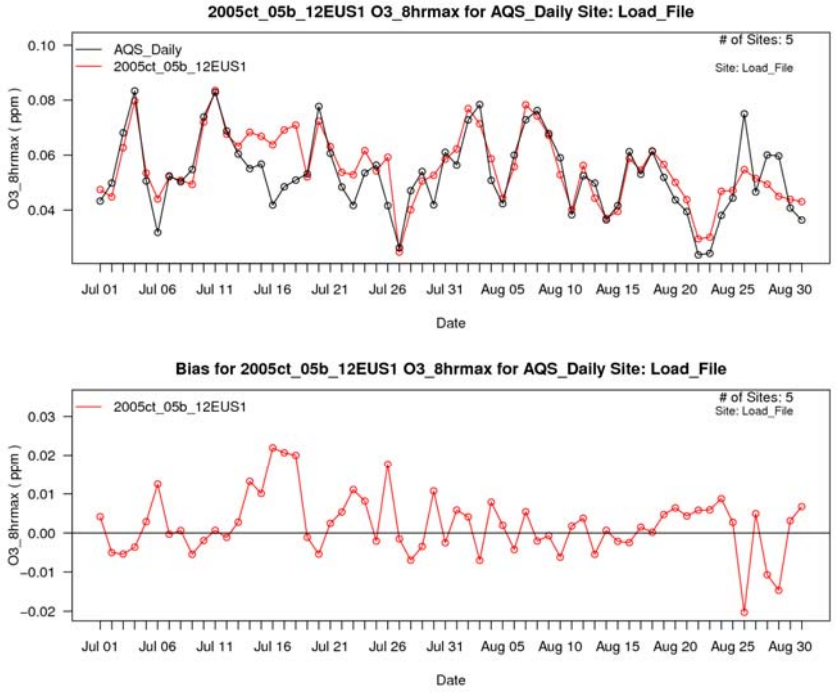

Figure 22: Time series of model performance for 8-hr daily maximum ozone concentrations at Detroit monitoring sites for July and August 2005. Observed values shown in black and modeled values shown in red.

A.3. CHOICE OF SENSITIVITY CUTPOINTS

As described in Section 3.2.3, the multi-step adjustment technique applies sensitivities from HDDM/CMAQ runs performed under different emissions scenarios to cover the entire range of emissions reductions. The base sensitivity was used over the first 40% of NO_x reductions, the sensitivity from a simulation performed with 50% anthropogenic NO_x emissions was used over the next 35% of NO_x reduction and finally the sensitivity from a simulation performed with 75% anthropogenic NO_x emissions was used over the final 25% of NO_x reductions. An evaluation was performed to determine the ideal cut points to switch to the sensitivity derived from a different simulation.

First, HDDM estimates of ozone concentrations for 50% NO_x emissions cuts were compared to brute force simulations in which emissions NOx emissions were reduced by 50% and the model was rerun. The HDDM-predicted ozone concentration was calculated using Equations (5) and (9) – (12), with P = 50%. This analysis was repeated 51 times with X varying between 0 and 50 and Y= 100 –X (e.g. X=0 and Y = 50; X= 1 and Y = 49; X = 2 and Y = 48 etc). For each of the 51 iterations, the HDDM estimates of hourly ozone concentrations were compared to the modeled ozone concentrations from the brute force simulation. For each comparison a variety of performance metrics were calculated at the grid cells containing the eight Detroit monitoring sites, at the grid cells containing the ten Atlanta monitoring sites, and at the grid cells containing all AQS sites in the Eastern modeling domain. The calculated metrics include: mean bias, mean error, maximum bias, maximum error, 99^{th} percentile bias, 99^{th} percentile error, correlation coefficient (R), slope for the line of best fit, and intercept for the line of best fit. The maximum and 99^{th} percentile bias and error metrics were included to characterize the worst performance for HDDM when compared to brute force model simulations. For each of the bias and error metrics, the best performance occurs when the value of the metric is closest to zero. For R, values closest to one indicate the best performance. And for the line of best fit, a slope close to one and intercept close to zero indicates good agreement between HDDM predictions and brute force estimates. After evaluating the performance based on these nine metrics for these three subsets of model grid cells, it was determined that X=40% provided HDDM estimates that were closest to brute force estimates across multiple locations.

To determine best values for Y and Z, a similar analysis was done in which HDDM and brute force estimates of ozone at 75% NO_x cut and 100% NO_x cut conditions were compared. In both sets of analyses, X=40%, Y varied between 10% and 35%, and Z was set to 100 – (X+Y). Again, the nine metrics listed above were calculated to characterize how well HDDM estimates of ozone at these NO_x emissions levels compared to brute force model simulations for grid cells in Detroit, Atlanta, and across the eastern United States. Based on the relative

performance for the 9 metrics in these comparisons, Y = 35% and Z = 25% were deemed the most appropriate values for replicating brute force CMAQ simulations.

A.4. BRUTE FORCE VERSUS HDDM FOR 1-STEP AND 3-STEP APPLICATION OF HDDM SENSITIVITIES

As discussed previously, only the sensitivities from the base CMAQ/HDDM simulation were used to estimate ozone concentrations that would result from VOC reductions. Figure 23 and Figure 24 show a comparison of predicted ozone at 100% anthropogenic VOC reductions for the grid cells containing the Atlanta and Detroit monitoring sites respectively. These plots are density scatter plots: the y-axis shows the predicted ozone concentration using HDDM sensitivities, the x-axis shows the predicted ozone concentration using a brute force CMAQ simulation, and the colors represent the percentage of points which fall at any location on the plot. When the majority of points fall on the 1-to-1 line, as in Figure 23 and Figure 24, this indicates that the two techniques are estimating the same values. Figure 23 and Figure 24 demonstrate an excellent ability of the HDDM to replicate 100% VOC cuts from the brute force simulation. Plots comparing HDDM to brute force for the 50% VOC cut show even better agreement and are provided in Section Appendix B. Plots showing the change in ozone from the base simulation (100% of anthropogenic VOC emissions present) to 50% or 100% VOC cut scenarios also show similarly good agreement and are also provided in Section Appendix B.

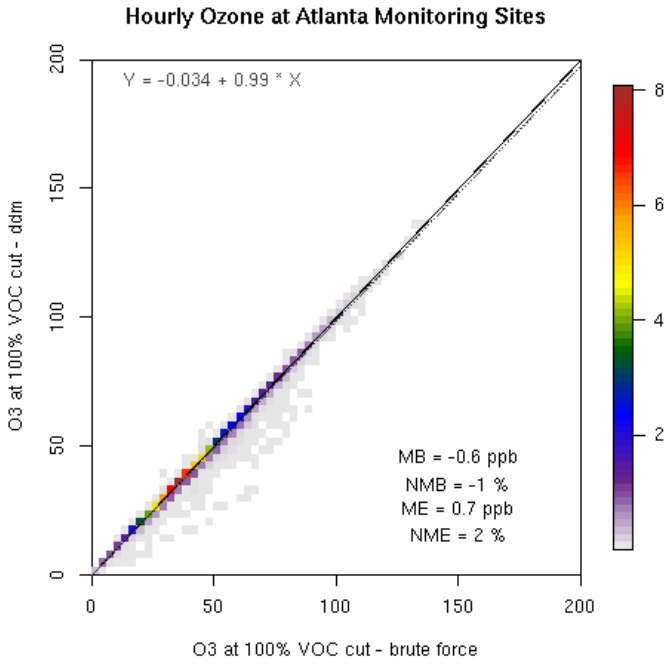

Figure 23: Comparison of HDDM to brute force ozone predictions with 100% VOC emissions cuts at grid cells containing Atlanta monitoring sites. Colors denote the percentage of points which fall in each location in this plot.

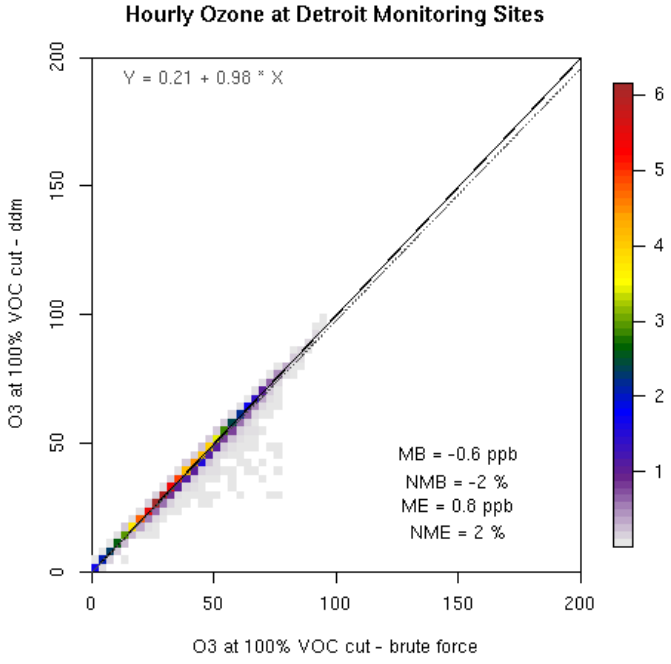

Figure 24: Comparison of HDDM to brute force ozone predictions with 100% VOC emissions cuts at grid cells containing Detroit monitoring sites. Colors denote the percentage of points which fall in each location in this plot.

Figure 25a, Figure 26a, Figure 27a, and Figure 28a show comparisons of predicted ozone using HDDM with sensitivities from the base runs only (1-step HDDM) to brute force CMAQ estimates at 75% and 100% anthropogenic NO_x reductions for the grid cells containing the Atlanta and Detroit monitoring sites respectively. These plots show considerably more scatter than the VOC reduction plots for 50% or 100% emissions cuts. Figure 25b, Figure 26b, Figure 27b, and Figure 28b show the same comparison except using multi-step HDDM calculations (2-step HDDM estimates for the 75% NO_x cut case and 3-step HDDM estimates for the 100% NO_x cut case). Comparing Figure 25a, Figure 26a, Figure 27a, and Figure 28a with Figure 25b, Figure 26b, Figure 27b, and Figure 28b shows that using sensitivities from multiple CMAQ/HDDM simulations over varying NO_x emissions levels provides ozone estimates that are in substantially better agreement with brute force emissions reductions CMAQ simulations. Even for the hypothetical case in which 100% of the anthropogenic NO_x emissions were eliminated, the 3-step HDDM ozone estimates only have a normalized mean bias of -15% in Atlanta and -0.9% in Detroit and normalized mean error of 31% in Atlanta and 13% in Detroit. Plots showing the change in ozone from the base simulation (100% of anthropogenic NO_x emissions present) to the 100% NO_x cut scenario are provided in Appendix B and show similarly improved performance when the 3-step application of HDDM sensitivities is used.

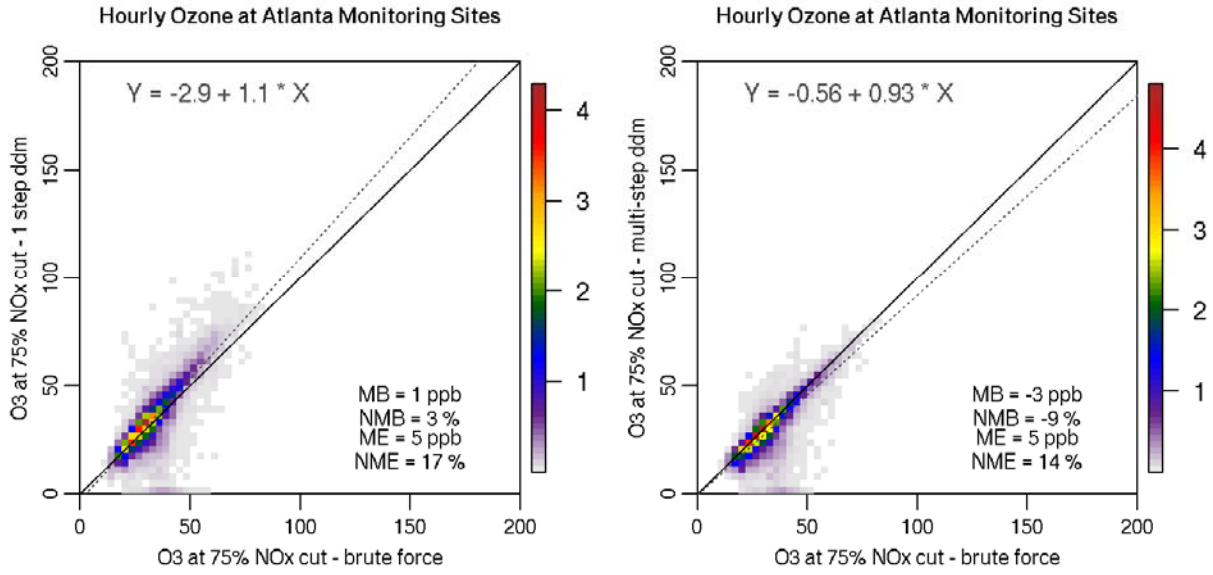

Figure 25: Comparison of 1-step (left) and multi-step (right) HDDM to brute force ozone predictions with 75% NO_x emissions cuts at grid cells containing Atlanta monitoring sites. Colors denote the percentage of points which fall in each location in this plot.

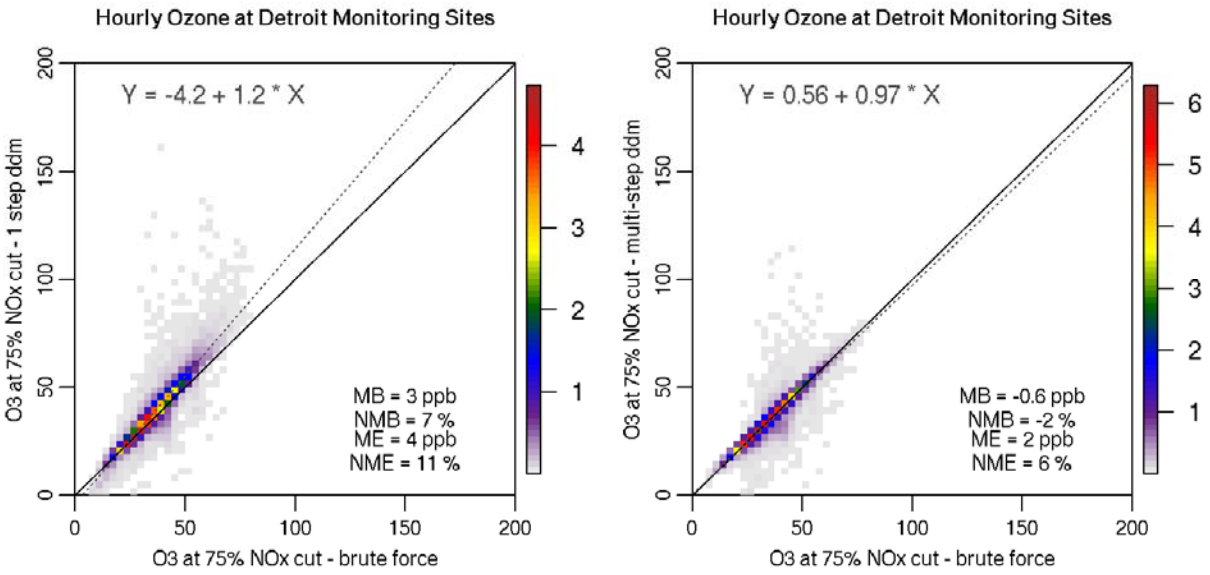

Figure 26: Comparison of 1-step (left) and multi-step (right) HDDM to brute force ozone predictions with 75% NO_x emissions cuts at grid cells containing Detroit monitoring sites. Colors denote the percentage of points which fall in each location in this plot.

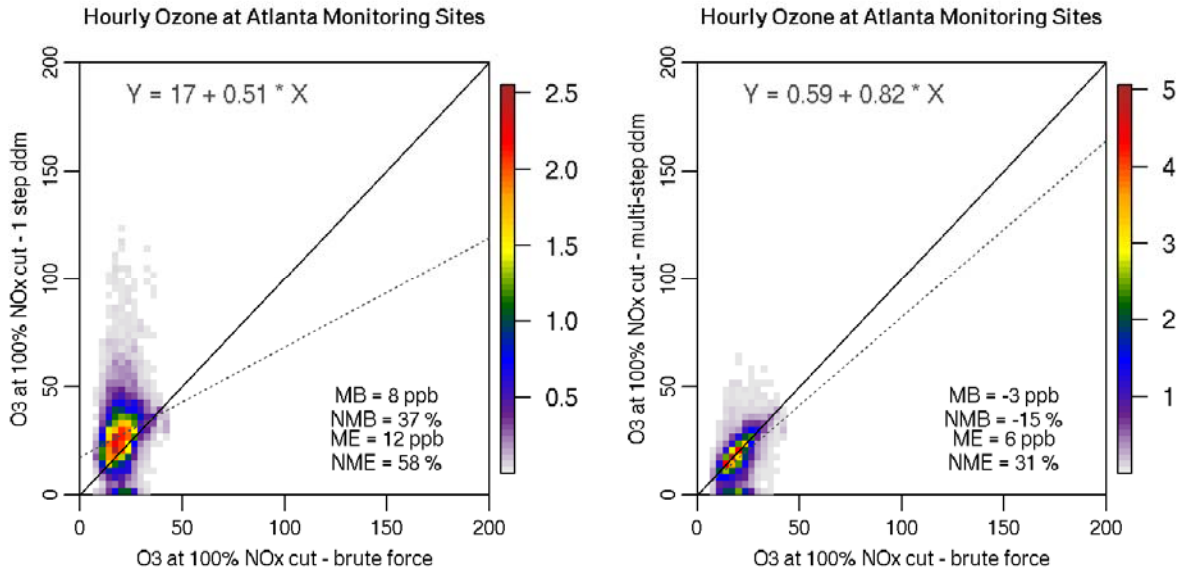

Figure 27: Comparison of 1-step (left) and multi-step (right) HDDM to brute force ozone predictions with 100% NO_x emissions cuts at grid cells containing Atlanta monitoring sites. Colors denote the percentage of points which fall in each location in this plot.

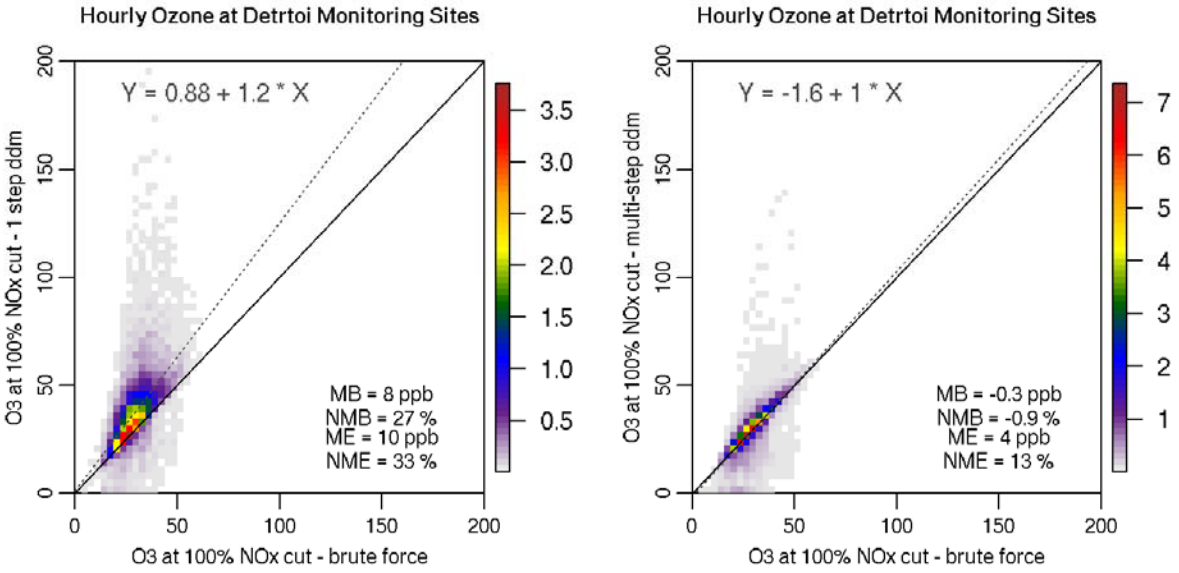

Figure 28: Comparison of 1-step (left) and multi-step (right) HDDM to brute force ozone predictions with 100% NO_x emissions cuts at grid cells containing Detroit monitoring sites. Colors denote the percentage of points which fall in each location in this plot.

APPENDIX B. ADDITIONAL PLOTS

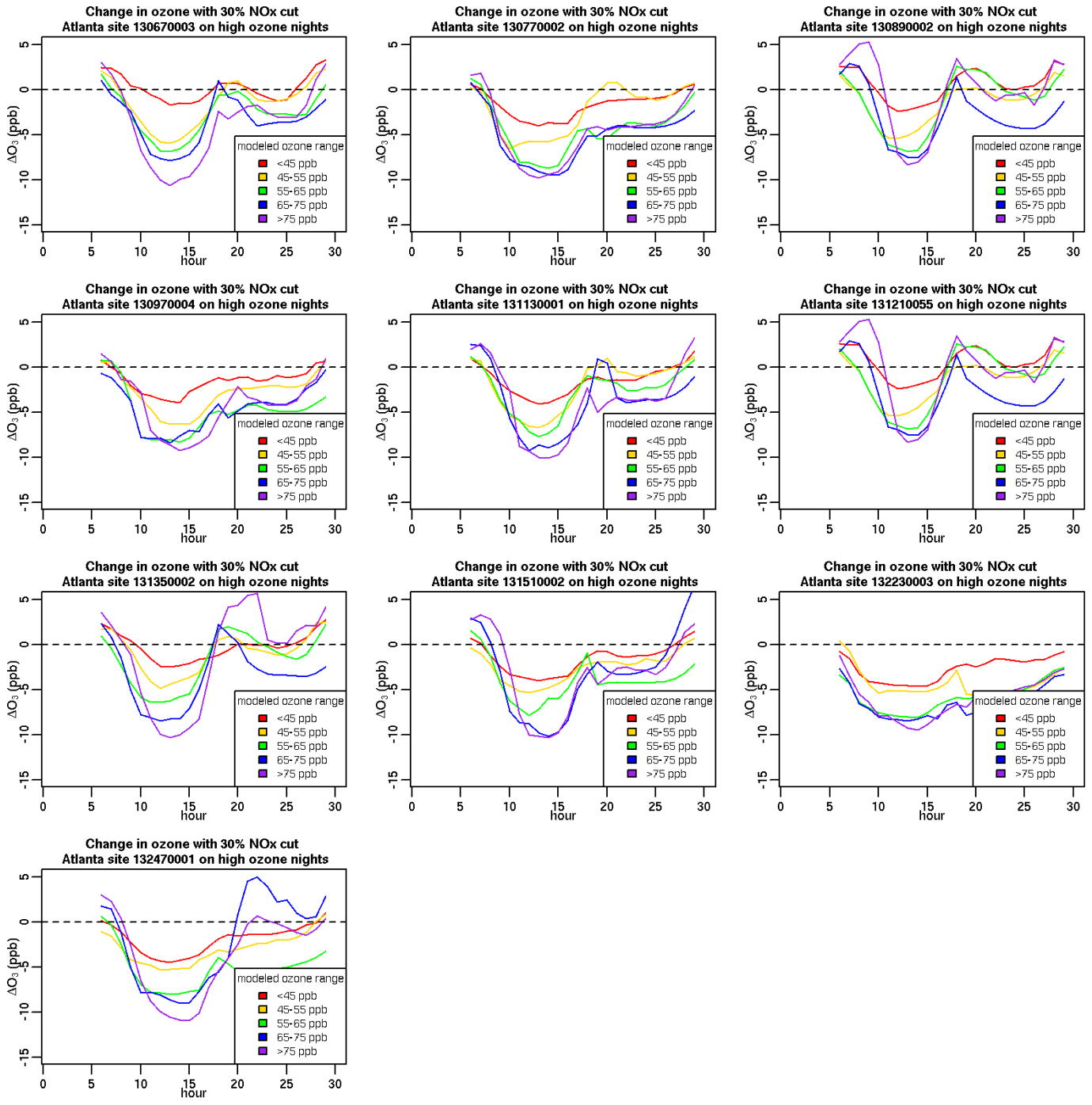

Figure 29: Predicted change in ozone concentrations (ppb) at all Atlanta sites with a 30% decrease in US anthropogenic NOx emissions in the Eastern US domain based on bins created for high ozone nights.

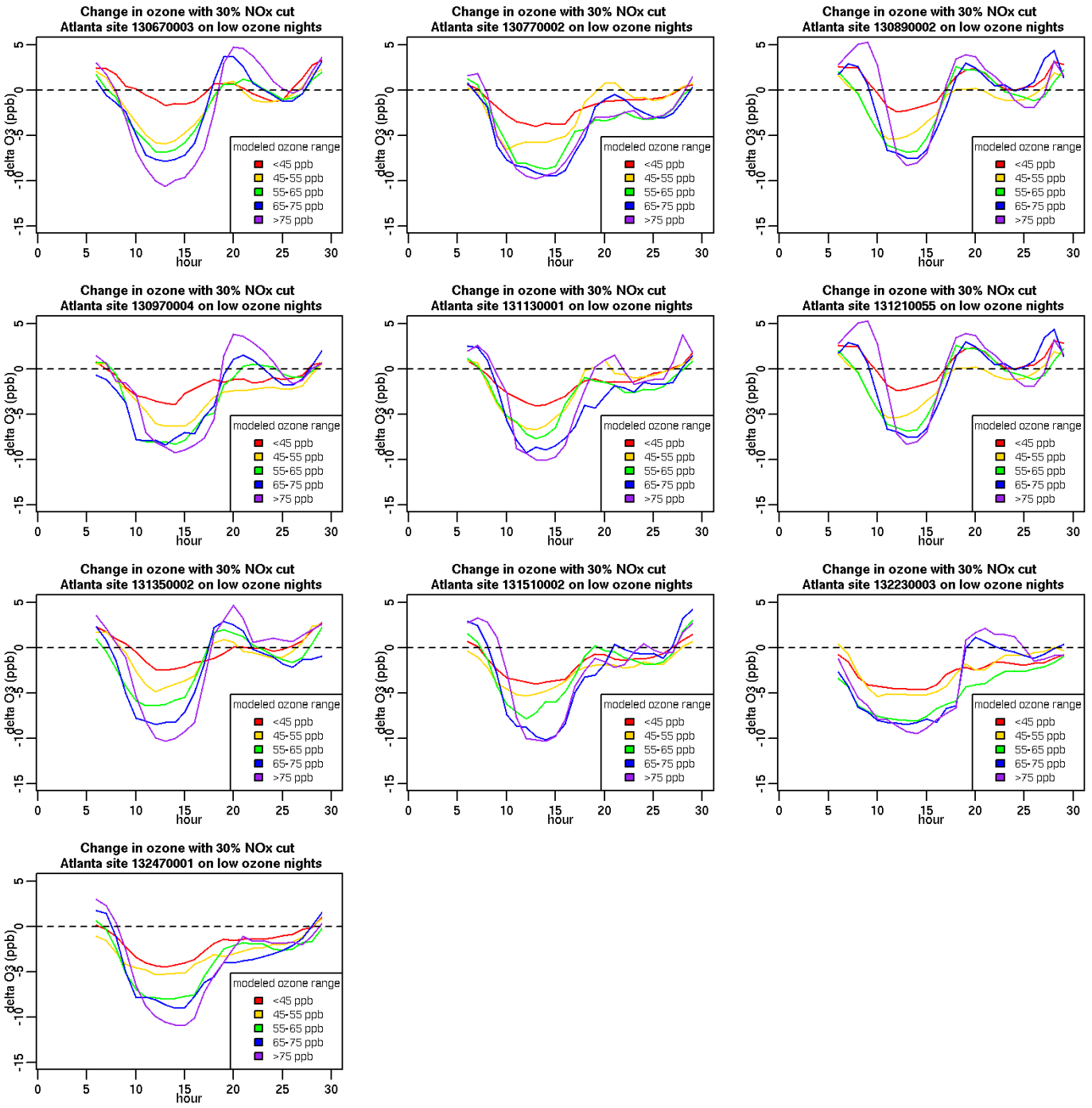

Figure 30: Predicted change in ozone concentrations (ppb) at all Atlanta sites with a 30% decrease in US anthropogenic NOx emissions in the Eastern US domain based on bins created for low ozone nights.

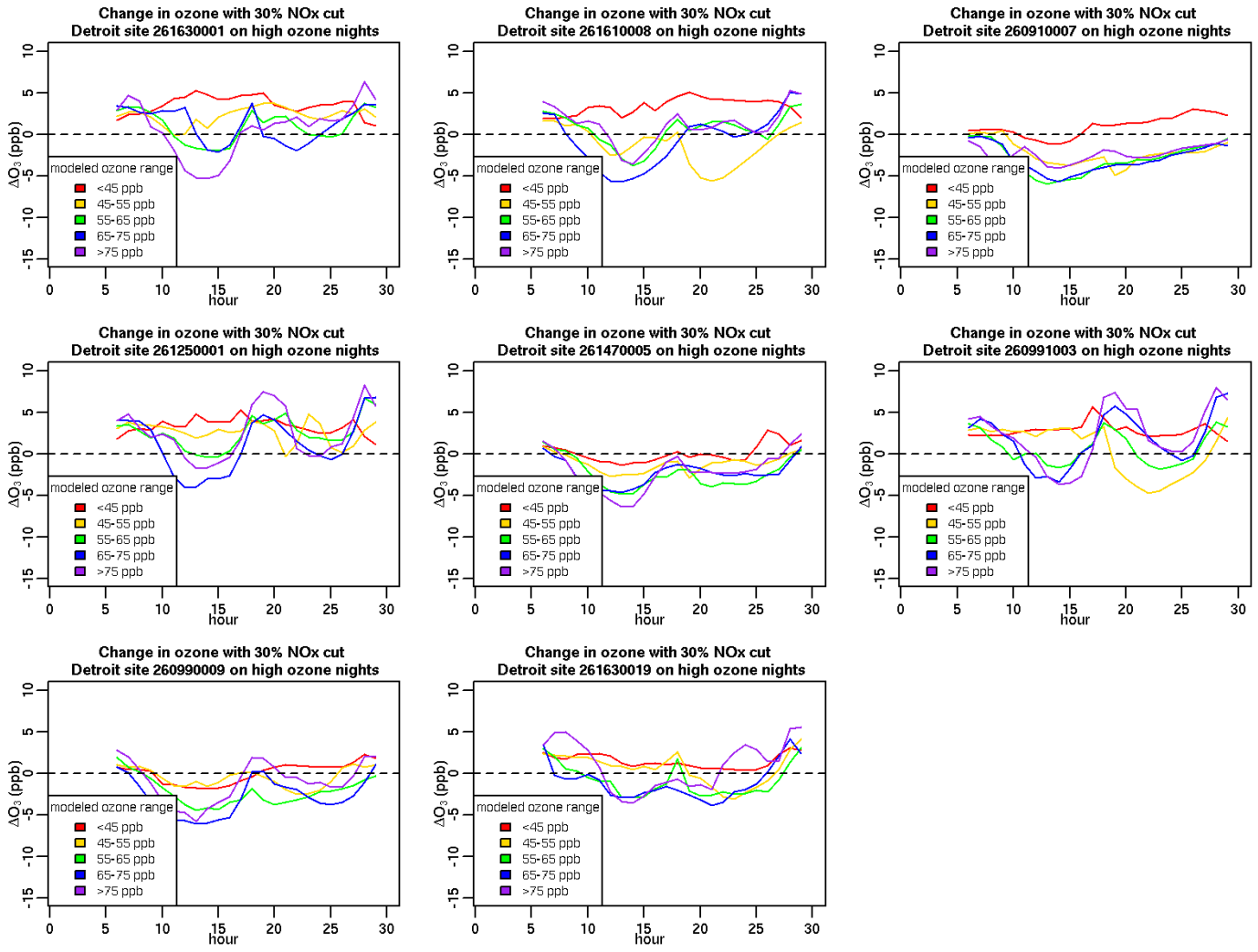

Figure 31: Predicted change in ozone concentrations (ppb) at all Detroit sites with a 30% decrease in US anthropogenic NOx emissions in the Eastern US domain based on bins created for high ozone nights.

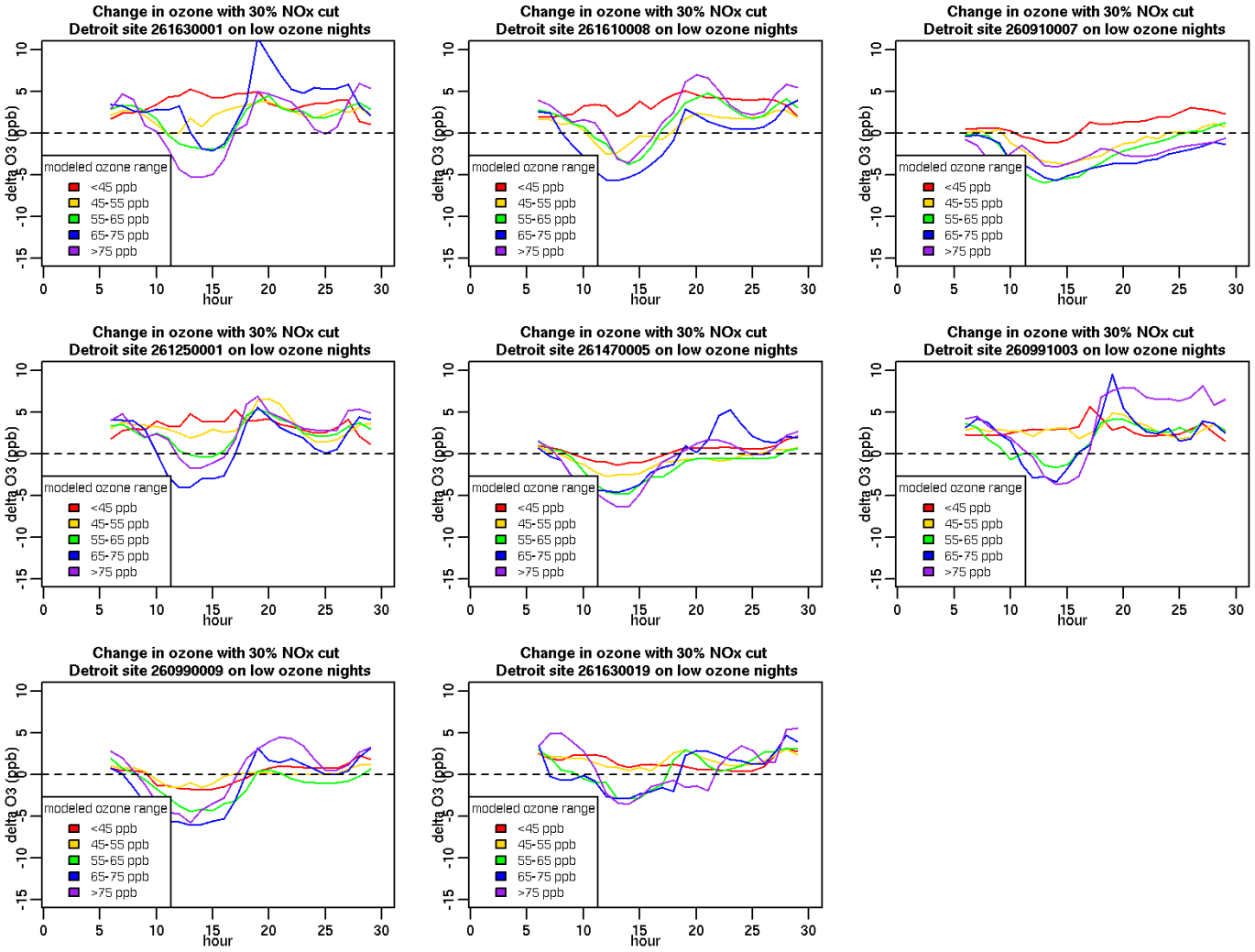

Figure 32: Predicted change in ozone concentrations (ppb) at all Detroit sites with a 30% decrease in US anthropogenic NOx emissions in the Eastern US domain based on bins created for low ozone nights.

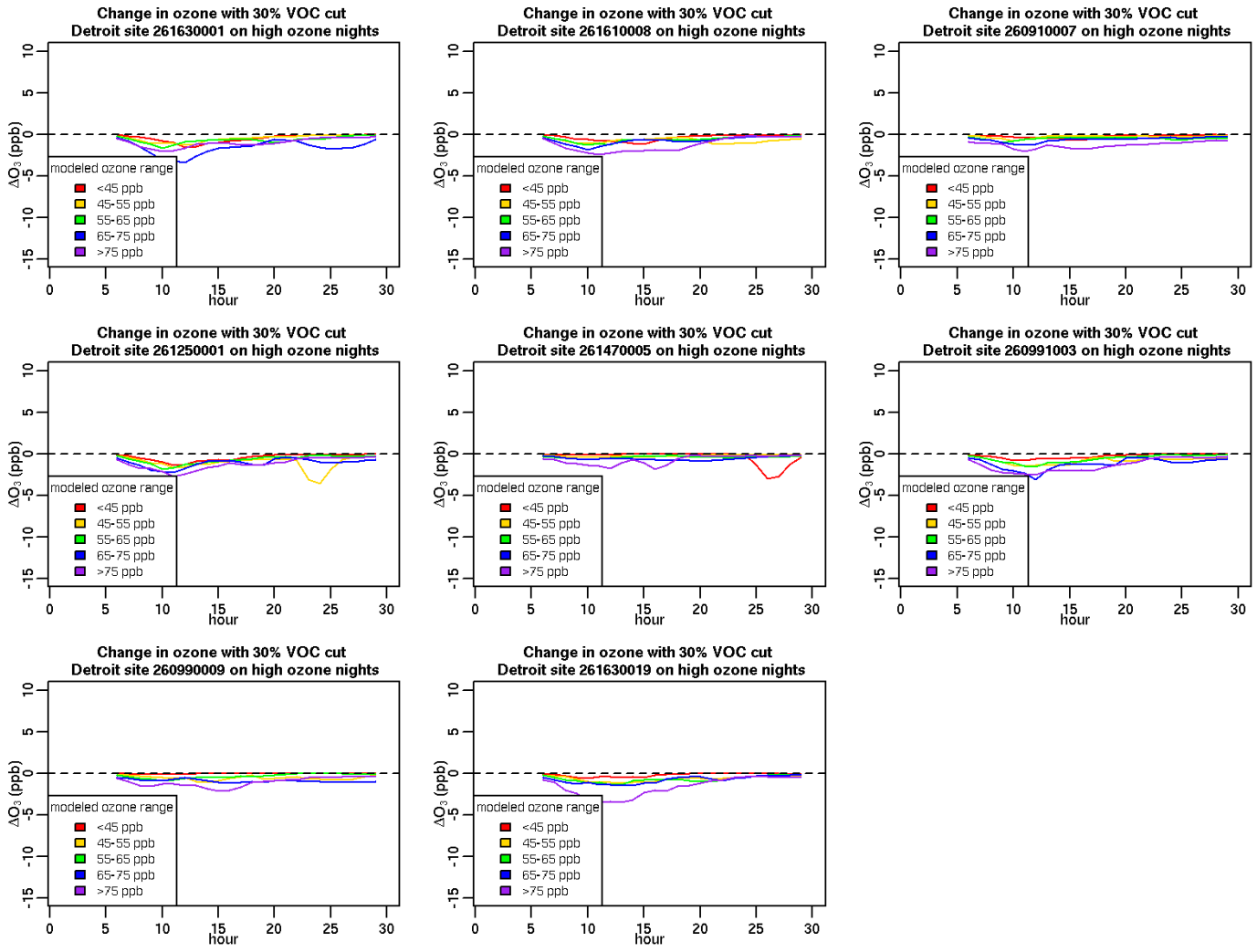

Figure 33: Predicted change in ozone concentrations (ppb) at all Detroit sites with a 30% decrease in US anthropogenic VOC emissions in the Eastern US domain based on bins created for high ozone nights.

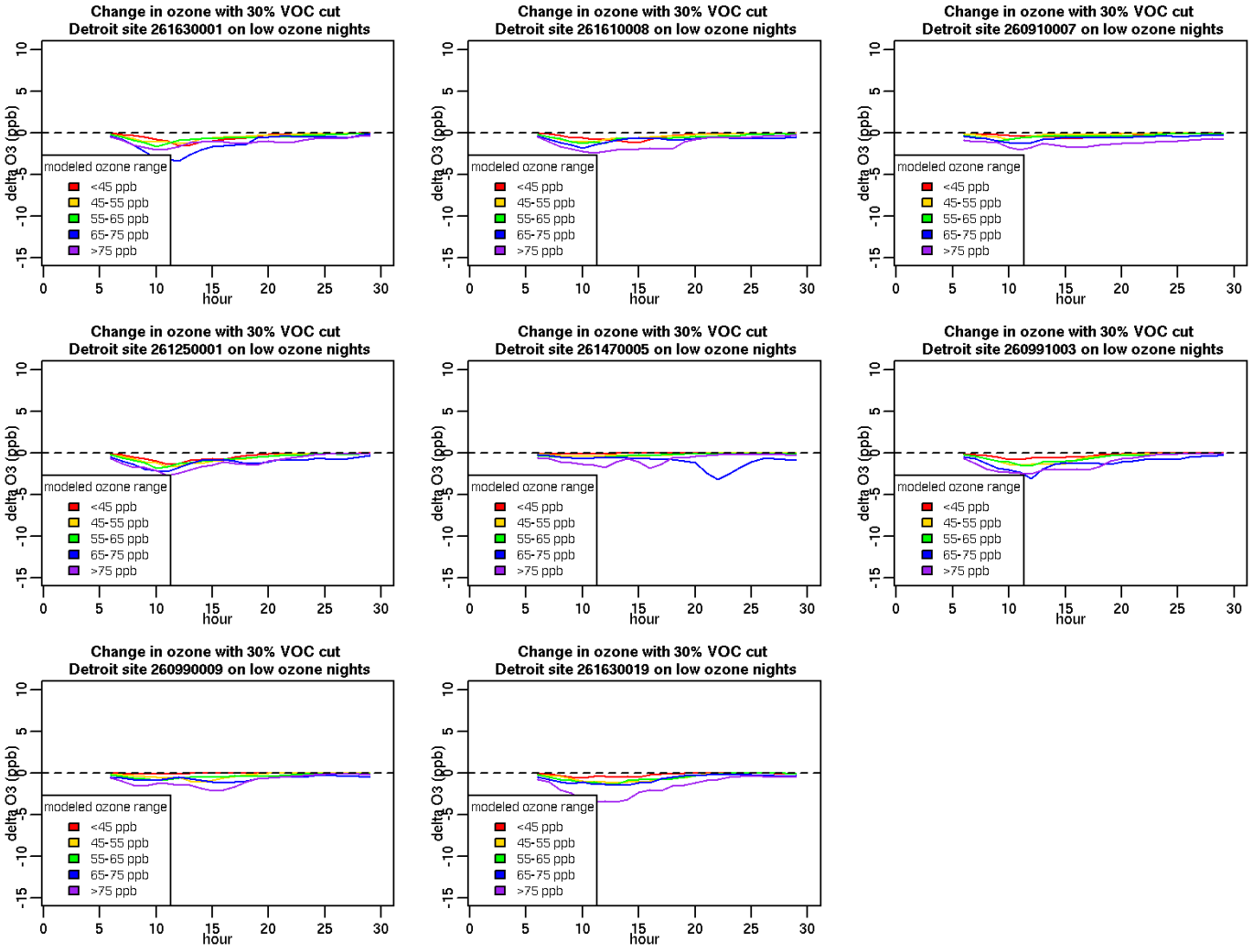

Figure 34: Predicted change in ozone concentrations (ppb) at all Detroit sites with a 30% decrease in US anthropogenic VOC emissions in the Eastern US domain based on bins created for low ozone nights.

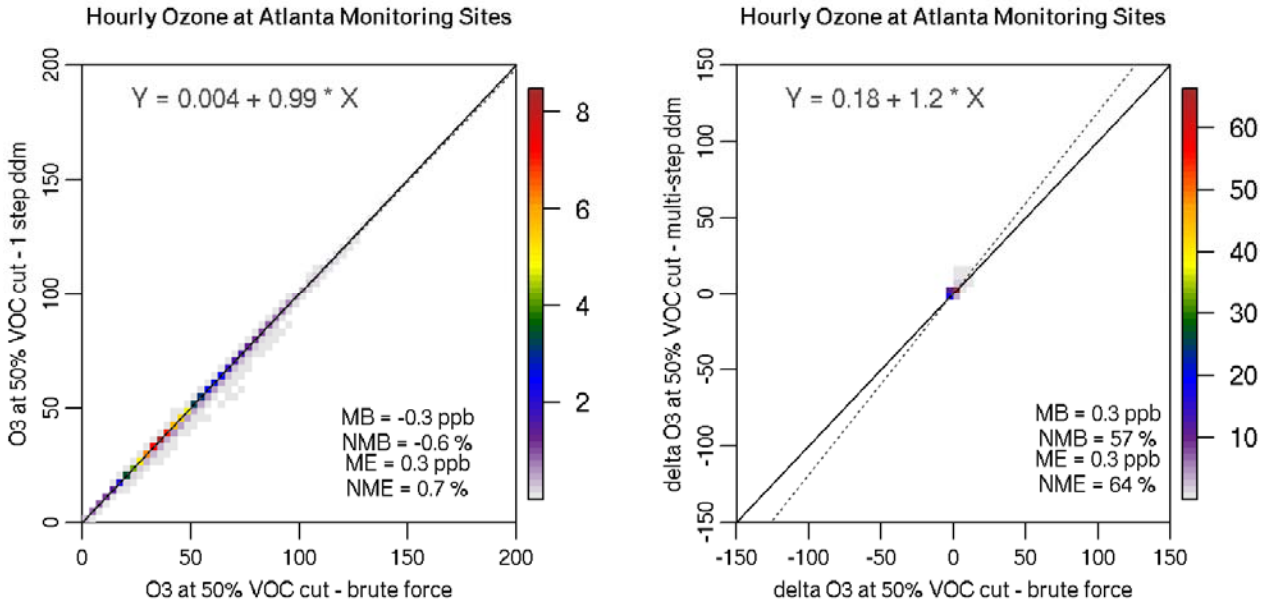

Figure 35: Comparison of 1-step HDDM to brute force ozone concentrations (left) and changes in ozone (right) due to 50% eastern US VOC emissions cuts at grid cells containing Atlanta monitoring sites. Colors denote the percentage of points which fall in each location in this plot.

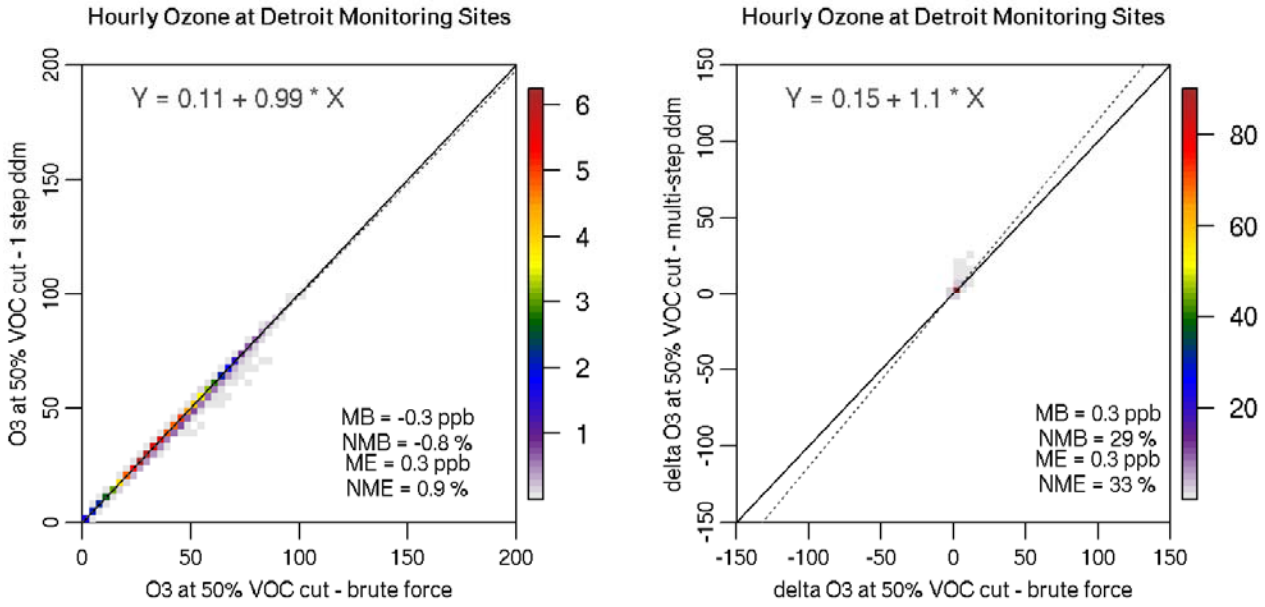

Figure 36: Comparison of 1-step HDDM to brute force ozone concentrations (left) and changes in ozone (right) due to 50% eastern US VOC emissions cuts at grid cells containing Detroit monitoring sites. Colors denote the percentage of points which fall in each location in this plot.

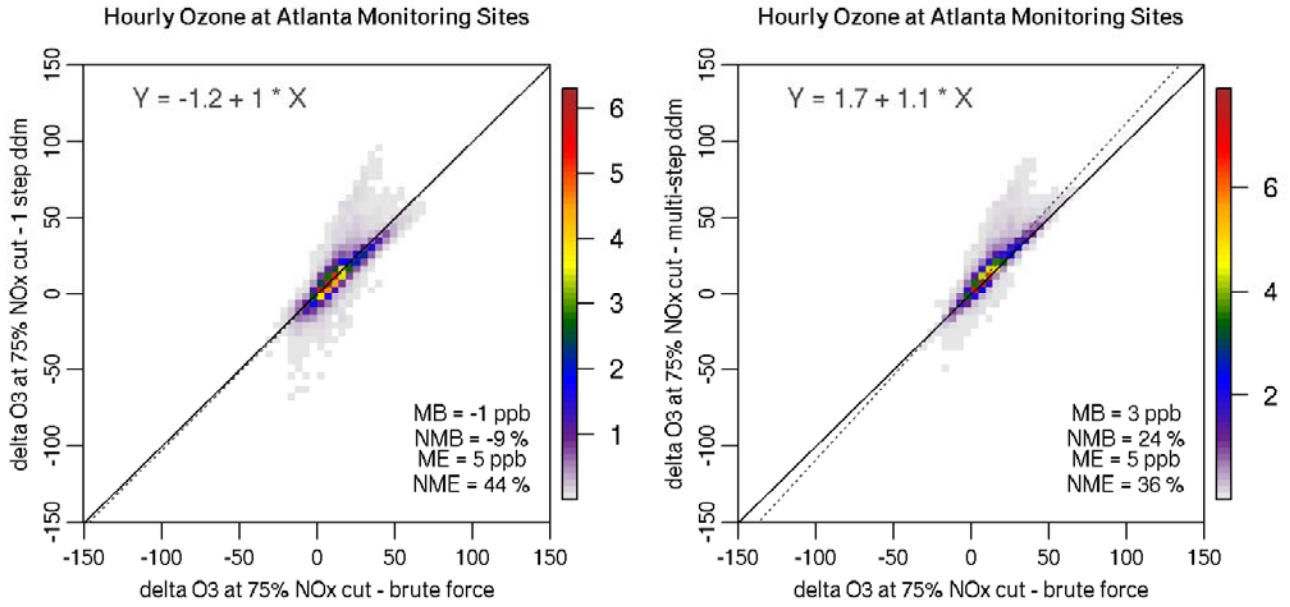

Figure 37: Figure 34: Comparison of 1-step (left) and multi-step (right) HDDM to brute force changes in ozone due to 75% NOx cuts at grid cells containing Atlanta monitoring sites. Colors denote the percentage of points which fall in each location in this plot.

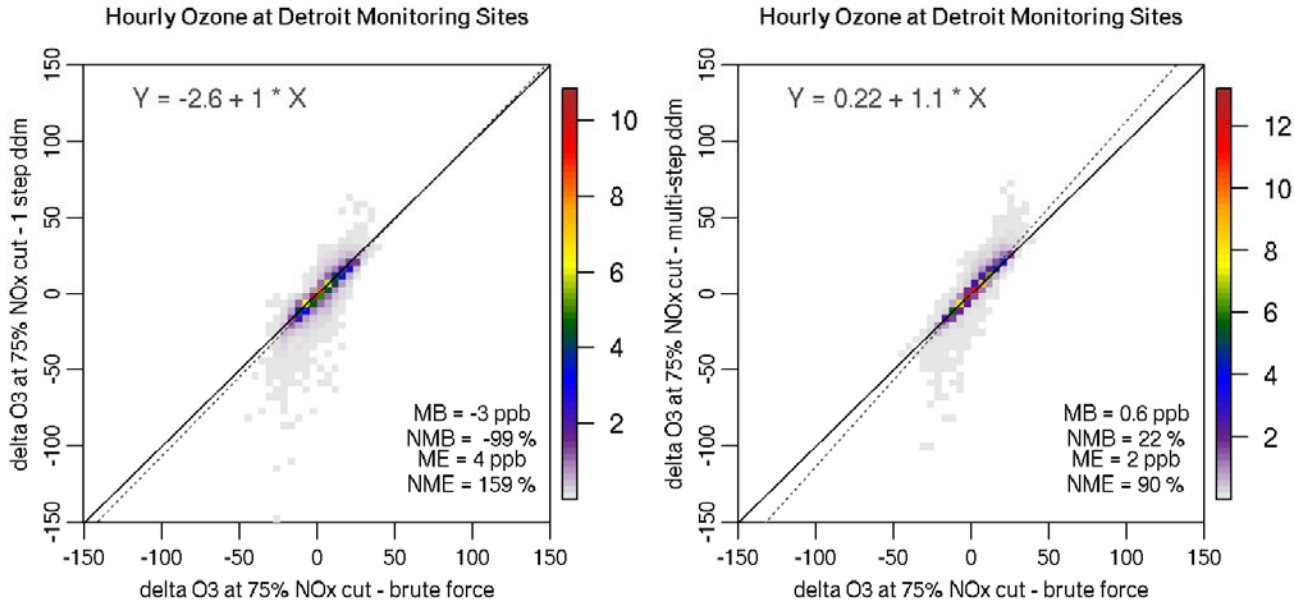

Figure 38: Figure 34: Comparison of 1-step (left) and multi-step (right) HDDM to brute force changes in ozone due to 75% NOx cuts at grid cells containing Detroit monitoring sites. Colors denote the percentage of points which fall in each location in this plot.

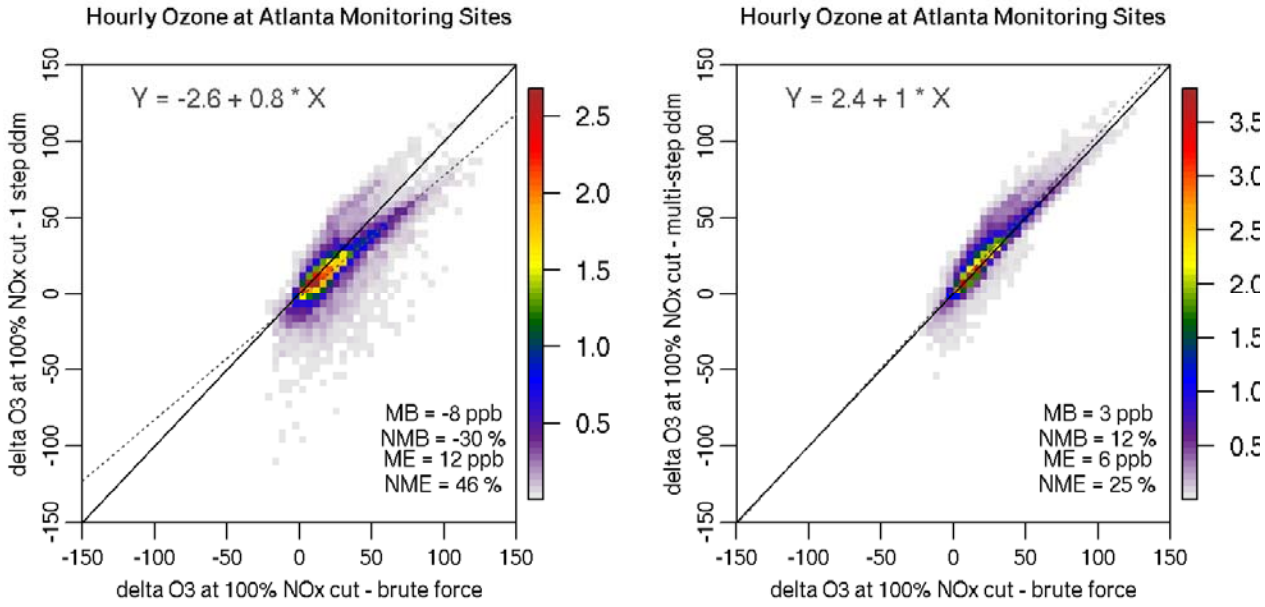

Figure 39: Figure 34: Comparison of 1-step (left) and multi-step (right) HDDM to brute force changes in ozone due to 100% NOx cuts at grid cells containing Atlanta monitoring sites. Colors denote the percentage of points which fall in each location in this plot.

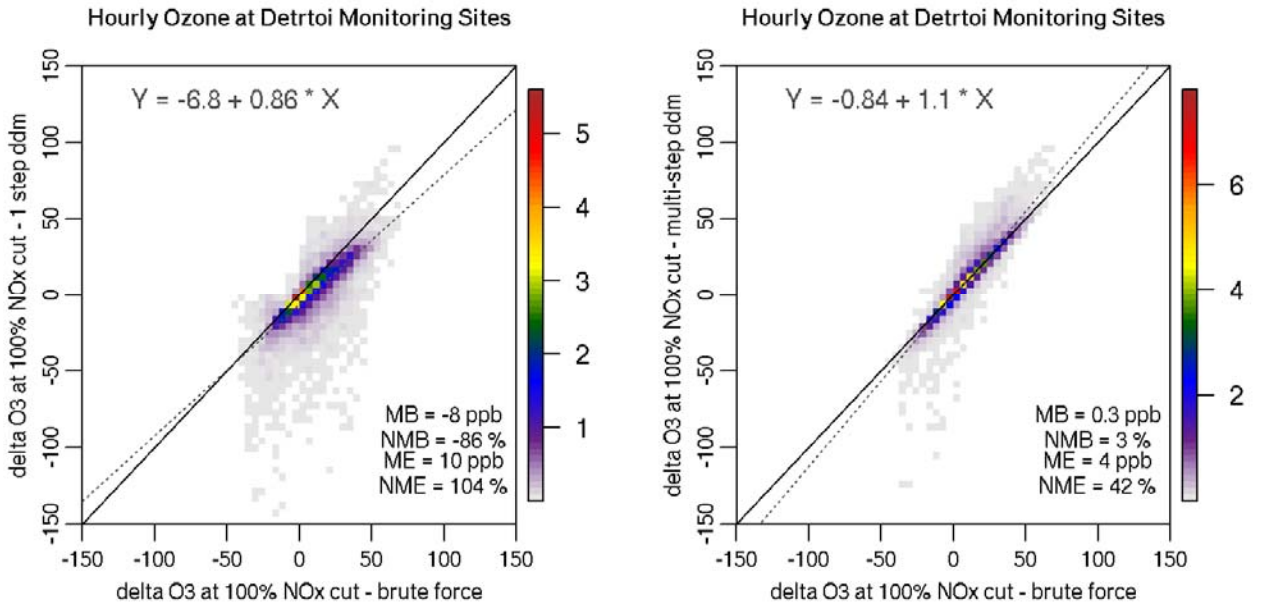

Figure 40: Comparison of 1-step (left) and multi-step (right) HDDM to brute force changes in ozone due to 100% NOx cuts at grid cells containing Detroit monitoring sites. Colors denote the percentage of points which fall in each location in this plot.

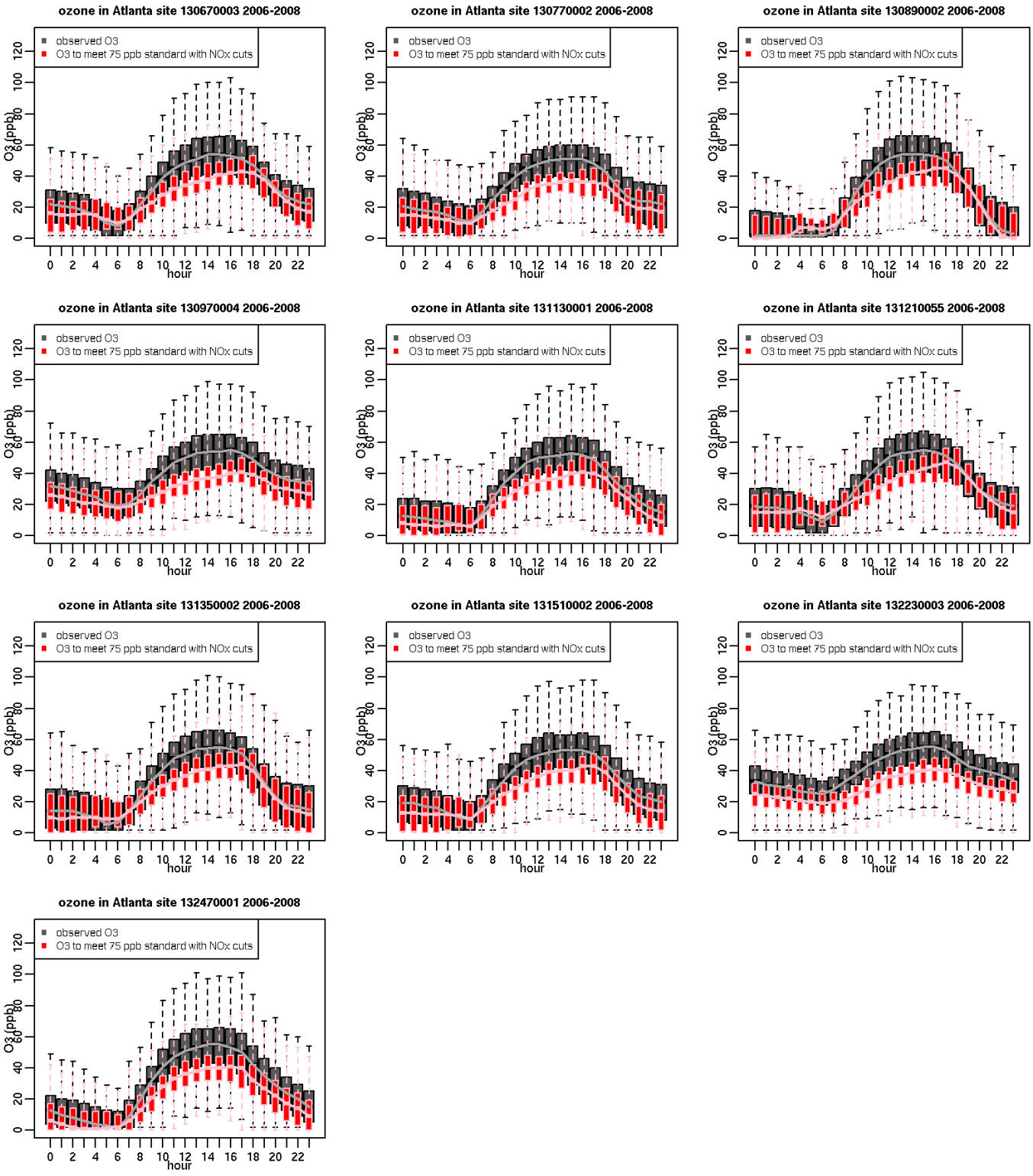

Figure 41: Distribution of ozone concentrations by hour of day at each Atlanta monitoring site. Centerlines show median values, boxes designate 25th to 75th percentile values and whiskers extend to 1.5 times the interquartile range. Values in

gray/black show measured ozone distributions (2006-2008) and values in red/pink show predicted ozone distributions based on HDDM model-based adjustment approach (2006-2008)

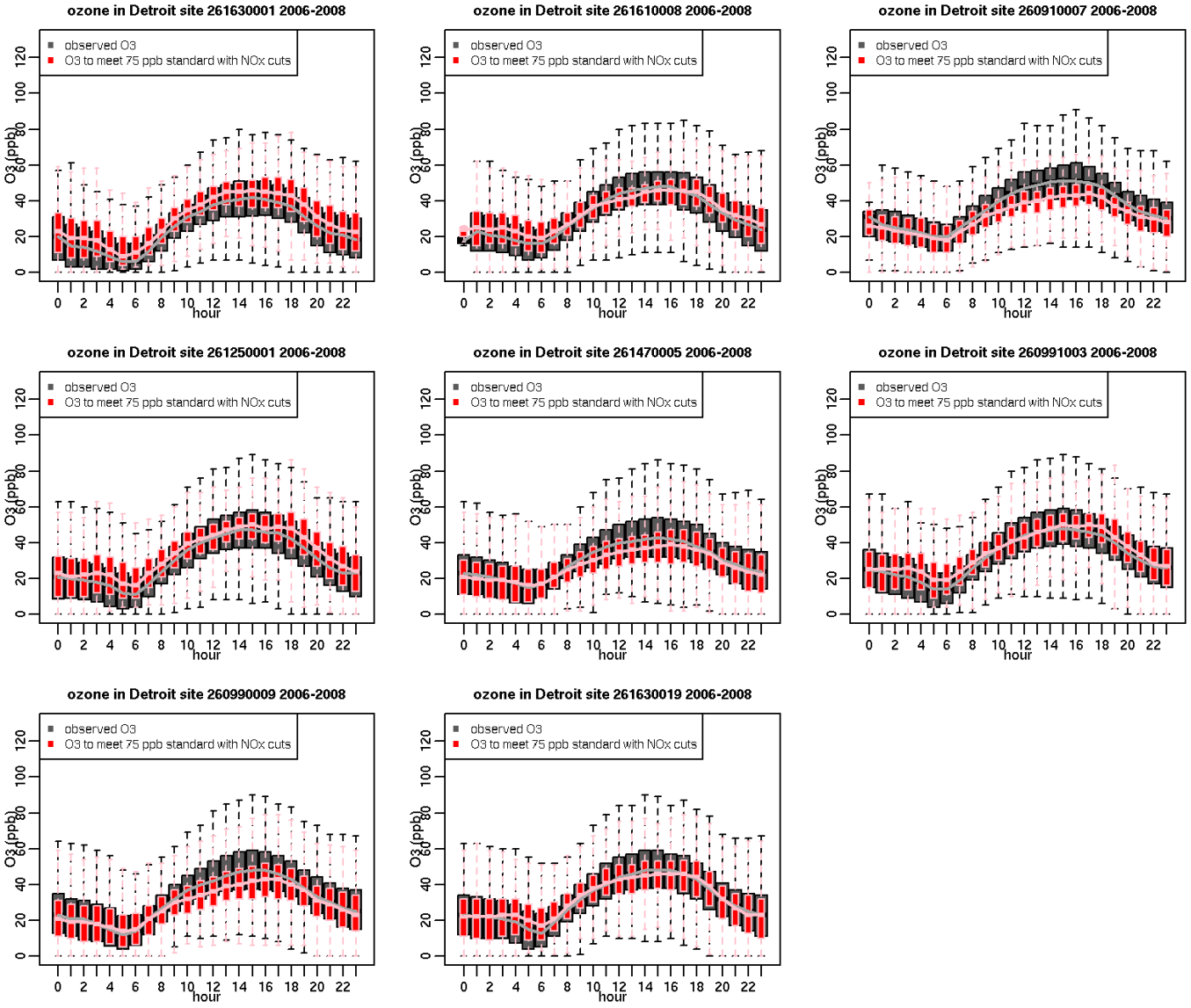

Figure 42: Distribution of ozone concentrations by hour of day at each Detroit monitoring site. Centerlines show median values, boxes designate 25th to 75th percentile values and whiskers extend to 1.5 times the interquartile range. Values in gray/black show measured ozone distributions (2006-2008) and values in red/pink show predicted ozone distributions based on HDDM model-based adjustment approach (NOx cuts) (2006-2008)

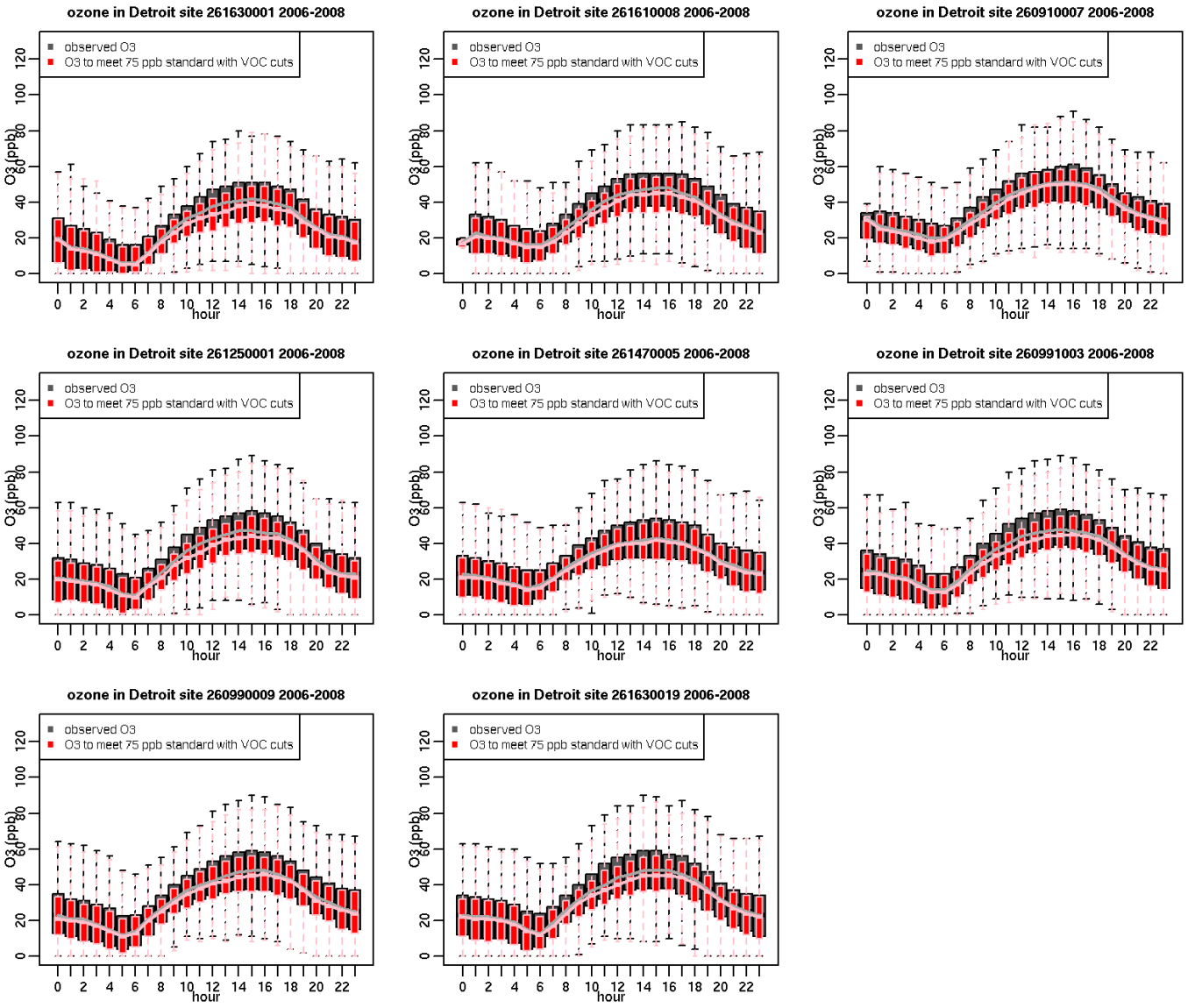

Figure 43: Distribution of ozone concentrations by hour of day at each Detroit monitoring site. Centerlines show median values, boxes designate 25th to 75th percentile values and whiskers extend to 1.5 times the interquartile range. Values in gray/black show measured ozone distributions (2006-2008) and values in red/pink show predicted ozone distributions based on HDDM model-based adjustment approach (VOC cuts) (2006-2008)